University of California
Santa Barbara

Computational Analysis of Acute Traumatic Coagulopathy

A dissertation submitted in partial satisfaction
of the requirements for the degree

Doctor of Philosophy
in
Mechanical Engineering

by

Tie Bo Wu

Committee in charge:

Professor Linda Petzold, Chair
Professor Jeff Moehlis
Professor Carl Meinhart
Dr. Mitchell Cohen

September 2019

The Dissertation of Tie Bo Wu is approved.

Professor Jeff Moehlis

Professor Carl Meinhart

Dr. Mitchell Cohen

Professor Linda Petzold, Committee Chair

August 2019

Computational Analysis of Acute Traumatic Coagulopathy

by

Tie Bo Wu

This dissertation is dedicated to my wonderful country, the United States of America, for welcoming me and my family as immigrants and giving us a chance at the pursuit of happiness.

Acknowledgements

All of science is a collaboration, and the work resulting in my PhD is no different. I owe my deepest gratitude to everyone who helped me in this journey. First and foremost, I would like to thank my PhD advisor, Linda Petzold, not only for the years of advice and guidance, but also for giving me a chance. None of this would be possible without her. I would also like to thank the rest of the committee: Jeff Moehlis, Carl Meinhart and Mitch Cohen for their time and advice.

I would like to thank my scientific collaborators, Mitch Cohen and the rest of the Denver team, Tom Orfeo and Kathleen Brummel-Ziedins, Jeff Varner and Rachel LeCover for their advice and insight. I would also like to thank Andri Bezzola and Sheng Wu for their help when I joined the lab. Without them, without them, I would have had nothing to build from. Especially Sheng, who wrote the PDE solver necessary to run my simulations.

I would like to thank the funding agencies and the American tax payers that ultimately funded my research.

I want to show my appreciation for all the friendships I've developed over my years at UCSB. I want to thank Ben Bales, Michael Trogdon, Kevin Deweese, Michael Agun, Arya Pourzanjani and Richard Jiang for the great times in and out of the office. I want to thank my fellow members of Whale Sharks Intramural Basketball, especially my classmates Jeff Peters, David Copp and Dan Wilson for the good times shared losing games to undergrads. I want to thank many of the other friends I've made during this time, Jeff Gopez, Dan Arnold, Collin Holgate, Lukas Dresel, the many volunteers and staff I met at the Santa Barbara Sea Center and many others. I want to thank my friends and family back home for always welcoming me back whenever I return home. They always make me feel like I never left. Lastly, I want to thank my loving girlfriend, Destinee, for all the support and care she gives me every day.

Curriculum Vitæ

Tie Bo Wu

Education

2019	Ph.D. in Mechanical Engineering (Expected), University of California, Santa Barbara.
2010	B.S. in Mechanical Engineering, Binghamton University - State University of New York

Awards

- **NSF IGERT Video and Poster Competition 2013: Judges' Choice Award Winner.** Project: 'Virtual Blood Vessels'. Competition to promote the understanding and dissemination of scientific ideas. Contestants were to create a short video and poster aimed to inform the general public about our particular research.

Publications

- Wu, T., Orfeo, T., Hunter, H.B., Sumislawwski, J.J., Cohen, M.J., Petzold, L.R. (2019) Computational Model of Tranexamic Acid on Urokinase Mediated Fibrinolysis. *In Preparation*
- Wu, T. B., Wu, S., Buoni, M., Orfeo, T., Brummel-Ziedins, K., Cohen, M., Petzold, L. (2018). Computational Model for Hyperfibrinolytic Onset of Acute Traumatic Coagulopathy. Annals of Biomedical Engineering., 1-10
- Pourzanjani A. A., Wu, T., Bales B.B., Petzold, L. R. (2018). Relating Disparate Measures of Coagulapathy Using Unorthodox Data: A Hybrid Mechanistic-Statistical Approach. StanCon 2018 Proceedings.
- Pourzanjani, A. A., Wu, T. B., Jiang, R. M., Cohen, M. J., Petzold, L. R. (2017, November). Understanding Coagulopathy using Multi-view Data in the Presence of Sub-Cohorts: A Hierarchical Subspace Approach. Machine Learning for Healthcare Conference Proceedings (pp. 338-351).
- Zhang, Y., Wu, T., Daigle, B. J., Cohen, M., Petzold, L.(2016). Identification of Disease States Associated with Coagulopathy in Trauma. *BMC Medical Informatics and Decision Making, 16*(1), 124.

Abstract

Computational Analysis of Acute Traumatic Coagulopathy

by

Tie Bo Wu

Over many millions of years of vertebrate evolution, our blood has developed a robust system to patch injuries and stop hemorrhage. However, sometimes a serious injury can derail this system completely. Acute Traumatic Coagulopathy (ATC) is a condition that arises often in major trauma that makes the cessation of bleeding an uphill battle, even with the help of modern medicine. Confounding properties of ATC include inefficacy of transfusion treatment, tissue specific hemostasis and time-sensitive efficacy of tranexamic acid. In addition, the mechanism or mechanisms behind ATC are still unresolved. Due to the complex nature of the coagulation system and limited methods for obtaining data, it is difficult to make progress with empirical experiments alone. Computational models offer a way to leverage our current understanding of coagulation to unravel the mystery of how ATC could occur.

In this thesis, we use computational models to propose a mechanism for ATC through hyperfibrinolysis and provide a model that can be used to test other hypotheses. We propose that the fibrinolytic response, specifically the release of tissue-plasminogen activator (t-PA), within vessels of different sizes leads to a variable susceptibility to local coagulopathy through hyperfibrinolysis. This can explain many of the clinical observations in the early stages from severely injured coagulopathic patients. In addition, we simulate the efficacy of tranexamic acid treatment on coagulopathy initiated through endothelial t-PA release, and are able to reproduce the time-sensitive nature of the efficacy of this treatment as observed in clinical studies. We also provide a model which can simulate

empirical studies on current and future treatments to improve our understanding and to help develop new treatments.

Contents

Chapter 1

Introduction

Over millions of years, animals have developed a vascular system to deliver nutrients and oxygen to the cells in their bodies, with blood as the medium. This system has enabled animals to become larger and more complex, but also adds a vulnerability. For as long as blood as existed, so has death by hemorrhage. Because of this, blood has evolved to repair the vascular system on its own, through the complex process of blood coagulation. For all of human history, trauma has been a major cause of death, with hemorrhage as the primary mechanism. Today, in the United States trauma is the leading cause of death for people ages 1-44[1]. As technology has developed, the amount of ways to inflict trauma have only increased (guns, cars, stairs). Trauma is a problem that is not going away.

Treating trauma revolves around blood coagulation. Proper functioning of the coagulation system is absolutely essential for recovering from trauma. Even with all the advances in modern medicine, we still rely primarily on the body's coagulation system to stop hemorrhage. Most of the solutions we use to stop bleeding can be seen as ways of supporting or manipulating the coagulation system. Therefore, to understanding blood coagulation is critical to treating hemorrhage.

In this thesis, we use computational models to improve understanding of Acute Traumatic Coagulopathy(ATC), a condition that manifests in increased bleeding and resultant mortality [2]. The mechanisms underlying ATC are not yet fully understood. Since coagulation is such a complex network of reactions occuring in fluid flow in chmically active blood vessels, computational models allow us to test and generate hypotheses in a principled manner.

Chapter 2

Background

2.1 Coagulation Cascade

The network of reactions that occur during blood coagulation is often referred to as the coagulation cascade (Figure 2.1). The name is a good description of the phenomena because once the cascade is triggered, a long chain of reactions follow in sequence. The main chemical species in the coagulation cascade are called the coagulation factors, which belong to a class of proteins called zymogens. Zymogens are precursors to enzymes that are inactive until they become activated. These inactive proteins in the blood allow the blood to always be ready to coagulate, without spontaneously impeding blood flow. When a blood vessel is damaged, coagulation is initiated when blood becomes in contact with cells beneath the inner layer of the blood vessel (subendothelium), expressing a protein called tissue factor (TF). This triggers what is known as the extrinsic pathway of the coagulation cascade. This starts a sequence of reactions that result in the activation of prothrombin (II) to thrombin (IIa). The chain of reactions begins with TF activating factor VII, which in turn creates an enzyme complex that activates factors IX and X. This produces small amounts of thrombin (IIa) which in turn activates factors V and VIII.

This allows for the creation of two more enzyme complexes. Factors VIIIa and IXa form tenase which rapidly activates factor X, and factors Va and Xa form prothrombinase, which rapidly converts prothrombin to thrombin. Thrombin is often seen as the central component of the coagulation cascade as it is responsible for converting the inactive fibrinogen (Fg) in the blood into fibrin (Fn), a polymer mesh that is the main component of the clot. Thrombin also activates platelets, causing them to change shape from smooth discs to an irregular shape with tendrils, allowing them to stick to fibrin, which solidifies the clot.

Creating a localized clot to stop the bleeding is only one part of the coagulation cascade. If these activated proteins get carried downstream away from the injury site, they need to be quickly inhibited so that they do not cause blockages in the vasculature. Thus, the coagulation cascade also contains many negative feedback mechanisms so that the coagulation process is contained at the injury site. These inhibitors include tissue factor pathway inhibitor (TFPI), which inhibits TF complexes, anti-thrombin III (ATIII), which inhibits thrombin, activated protein C, which degrades factors Va and VIIIa. After the bleeding has stopped and the vessel is repaired, it is important that the clot that was once there can break down so that the blood vessel can return to its original state. The breakdown of the clot is a process known as fibrinolysis, which is carried out by the protein plasmin (Pn), which is activated as soon as the clot begins to form. Plasmin breaks down fibrin into small inactive fragments known as fibrin degradation products (FDP). Plasmin must then get de-activated by α2-antiplasmin (AP) so that future clots are allowed to form. The cascade ends with all of the active proteins deactivated. Over time, the kidneys will filter out the byproducts of the process and the liver will replenish the coagulation proteins that were used, so that the blood is returned to its original state.

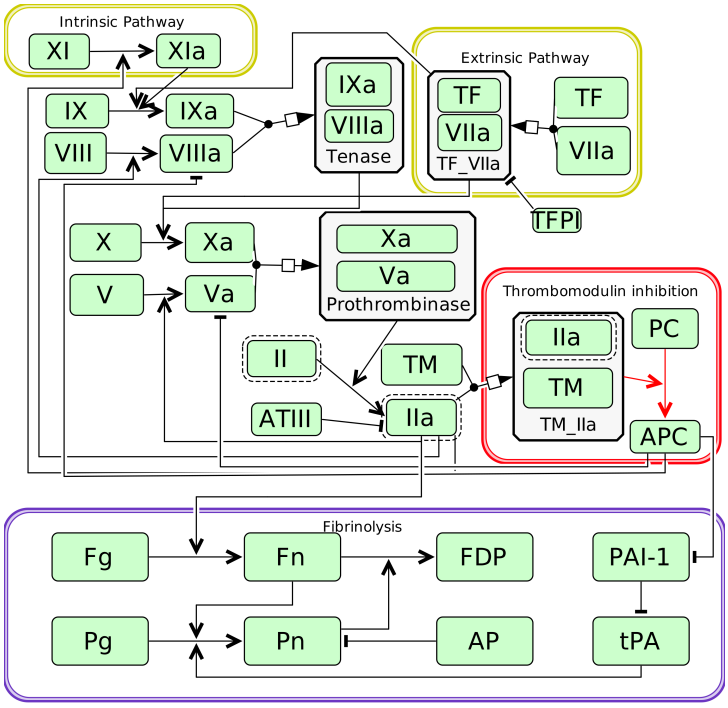

Figure 2.1: Simplified Diagram of Coagulation-Fibrinolysis System. Clotting factors become activated via the intrinsic and/or extrinsic pathway, which culminate in the production of thrombin (IIa). Thrombin then converts fibrinogen (Fg) to fibrin (Fn). The clot formed from fibrin is degraded by plasmin (Pn) which is converted from plasminogen (Pg) by tissue-plasminogen activator(tPA). Additional notation: TF(Tissue Factor), ATIII (Anti-Thrombin III), TFPI (Tissue Factor Plasma Inhibitor), TM (Thrombomodulin), IIa (Thrombin), PC (Protein C), APC (Activated Protein C), FDP (Fibrin Degradation Products), PAI-1 (Plasminogen Activator Inhibitor-1), AP (α_2-antiplasmin). Roman numerals represent the corresponding coagulation factors, and the letter "a" denotes that the factor is activated.

2.2 Coagulopathy

The coagulation system is not fail-proof; in some cases its ability to stop hemorrhaging can be hindered or even inhibited. Coagulopathy is the umbrella term for conditions that impair coagulation function. These can be hereditary such as hemophilia, self-imposed through blood thinning medications such warfarin, or it can arise spontaneously from trauma. These trauma-induced coagulopathies are poorly understood, can manifest in different ways, and can be difficult to treat.

This thesis focuses on acute traumatic coagulopathy (ATC), which arises in the early stages of trauma[3]. This condition results in severely impaired coagulation function and increased bleeding. Along with the primary symptom of impaired coagulation, there are some interesting characteristics of ATC. One of the main characteristics of ATC is the ineffectiveness of massive transfusions during treatment[4]. This raises an important question, if there is a problem with the blood, why does coagulopathy persist even after repeatedly replacing it? Another important characteristic is that often a patient will have tissue-specific hemostasis, meaning that different parts of the body will exhibit different clotting behaviors[5]. This not only tells us that ATC is a local phenomena, it also demonstrates how difficult it is to treat: if treatment to improve clotting is given to the patient, it needs to be targeted to the injury site or else it could cause clots to form in unwanted areas. Another interesting characteristic is how it responds to the anti-fibrinolytic drug tranexamic acid (TXA). If TXA is provided early, it appears to have good results, but if provided late, it becomes ineffective and sometimes detrimental[6]. We also know that ATC, often occurs in patients with blunt injuries and in conjunction with shock[7]. There have been many proposed hypotheses on the mechanism(s) behind ATC but they typically fail to explain all of the previously mentioned characteristics. These theories are primarily based on observational and anecdotal clinical data, which is often flawed or easy to misinterpret. The data that is available typically comes in a few forms. One type is protein data, which tells us which of the blood proteins correlate with patients with coagulopathy. Another type of data comes in the form of clinical measurements, which tells us which vital measurements (such as blood pressure, body temperature or heart rate) correlate with ATC. Anecdotal information such as the types of injuries that are more likely to lead to ATC can often be relevant. This information is valuable but there are many flaws with it that we must be cognizant of when making hypotheses.

The biggest flaw with observational data is the difficulty of drawing causal relationships from correlational data. There are many proteins and clinical measurements that are significantly high or low in ATC patients, but we don't know whether or not these trends in coagulation protein levels cause ATC, are caused by ATC or have no causal relationship at all. Clinical blood protein data has another major flaw from how it is collected. Usually it is collected from a location away from the injury site. Since coagulation is a local phenomena affecting a relatively small fraction of the patient's blood, abnormalities in the blood at the collection site would not be nearly as prominent as the blood at the injury site. Other flaws include nonuniform injury severity, injury location, collection sites, collection times, sampling, as well as a very coarse and irregular time resolution in data samples.

With so many flaws in the data, hypotheses that are developed often cherry-pick information for support and dismiss opposing evidence as flawed. Due to the unethical nature of experimenting on humans, validation experiments are often incomplete abstractions of the original setting. Thus, many of the proposed mechanisms of ATC have yet to be validated.

There are two primary modes for poor coagulation: (1) poor clot formation[8], and (2) excessive clot lysis[9, 10]. The proposed mechanisms underlying poor clot formation include factor depletion, hemodilution and increased expression of activated protein C[7]. While previous computational studies on ATC have performed detailed analysis on clot formation through coagulation factor depletion and dilution [11, 12, 13, 14], the same level of attention has not been given to modeling ATC through hyperfibrinolysis. These studies demonstrate the deleterious effects of dilution-inducing therapies but they do not address characteristics such as the inefficacy of mass transfusion or the localized nature of ATC. While it is likely that ATC is the result of both modes acting in tandem, we posit that excessive clot lysis is the driving mechanism behind many of the clinical phenotypes

exhibited by patients with ATC.

2.3 Computational Models

In situations in which obtaining empirical data is difficult, computational models can be useful tools for proposing and testing hypotheses. Computational models allow us to easily change the conditions of the simulation and to extract all of the measurements used in the model. With such a complex network of reactions, there are many possible ways to impair the coagulation system. However, with a computational model, we can test which of these mechanisms can realistically cause coagulation malfunction under the conditions we see in ATC.

Fortunately, most of the reactions involved in coagulation have been well studied [15, 12, 16, 17]. Due to computational constraints, different models compromise on the level of detail in differing parts of their model. Therefore, each computational model must be tailored to the problem that it is trying to solve. There are blood models that focus on blood flow [18, 19, 20], platelet dynamics[21] or the geometry of a clot as it forms or degrades[22, 16]. Our models focus on blood chemistry and reaction dynamics in both the blood and the endothelium together with fluid flow, which we believe is most applicable to ATC.

2.4 Law of Mass Action

To model the chemistry of the blood, we primarily use the Law of Mass Action. The law states that the rate of the reaction is directly proportional to the concentration(s) of

the reactant(s). For a simple one-step, reversible, elementary reactions such as:

$$A + B \rightleftharpoons C$$

, the rate of the reaction can be written as:

$$r_1 = k_1[A][B]$$

for the forward reaction and:

$$r_2 = k_2[C]$$

for the backwards equation, where r represents the reaction rate (in units of M/s), k represents the rate constant (in units of 1/M*s or 1/s) and A,B,C are the concentration values of the chemical species (in units of M). The rates of the reactions also tells us the rates at which the concentrations are changing so our system of differential equations will look like:

$$\frac{\mathrm{d}[A]}{\mathrm{d}t} = r_1 - r_2 = \frac{\mathrm{d}[B]}{\mathrm{d}t} = -\frac{\mathrm{d}[C]}{\mathrm{d}t}$$

2.5 Michaelis-Menten Kinetics

In biological reactions, there are many reactions involving proteins, which are large folded molecules in which the shape determines the rate of reaction or whether or not it will react at all. Often, enzymes are required to change the conformation of a protein before it is able to react. In this situation, the reaction is a multi-step process. The simplest form can be represented with 3 species, the enzyme E, the substrate S and the

product P. The reactions would take the form:

$$E + S \rightleftharpoons ES \rightharpoonup E + P$$

These three reactions require three kinetic constants to represent their rate. However, under certain conditions, such as the substrate greatly outnumbering the enzyme, we can use the Michaelis-Menten Approximation to reduce these three reactions to a single irreversible using only 2 kinetic constants. The reaction would be simplified to:

$$S \xrightarrow{E} P$$

and the rate of this reaction is determined by:

$$r_3 = \frac{k_{cat}[E][S]}{S + K_m}$$

This approximation is often used because these kinetic constants are easier to obtain (and therefore more available) than the ones necessary to model the system as three separate reactions.

Chapter 3

Modeling Acute Traumatic Coagulopathy Using a Spatial Model

Trauma is the leading cause of death between the ages of 1 and 44[1]. Major trauma often induces a coagulopathic state known as Acute Traumatic Coagulopathy (ATC) that manifests in increased bleeding and resultant mortality [2]. The mechanisms underlying ATC are not yet fully understood. In this paper we propose a mechanism that can produce some of the observed phenotypes in ATC patients, and investigate its viability and implications via a computational model.

The coagulation process is a complex network of reactions (Figure 2.1) in which an over-expression or deficiency in many different proteins could lead to the hemorrhaging exhibited by ATC patients. There exists a very well studied network of blood protein interactions from in vitro studies [15, 23, 24] and recent in vivo analysis of trauma patient data [4, 10]. However, a mechanistic understanding of ATC has remained elusive. Some of the confounding characteristics of the disease include persistence despite massive transfusion[4], tissue-specific coagulation profiles[5], and the time sensitive efficacy

of treatments such as tranexamic acid (TXA)[6].

To study ATC within a mechanistic framework, we introduce a partial differential equation model to simulate in vivo coagulation in blood vessels, and explore conditions that could provide a mechanistic explanation for the phenomena present in ATC. There are two primary modes for poor coagulation: (1) poor clot formation [8], and (2) excessive clot lysis[9, 10]. While previous computational studies on ATC have performed detailed analysis on clot formation through coagulation factor depletion and dilution[11, 12, 13, 14], the same level of attention has not been given to modeling ATC through hyperfibrinolysis. These studies astutely demonstrate the deleterious effects of dilution-inducing therapies but they do not address the cause of trauma-induced coagulopathy prior to resuscitation. While it is likely that ATC is the result of both modes acting in tandem and perhaps different modes dominating depending on the stage of the disease, we posit that excessive clot lysis is initially the dominant pathway leading to ATC.

To understand the causes of excessive lysis, our model focuses on tPA (tissue-plasminogen activator), one of the primary proteins involved in fibrinolysis. It converts the inactive zymogen plasminogen into the active serine protease plasmin, which breaks down fibrin clots[25]. The concentration of tPA must be delicately balanced, as insufficient tPA can lead to thrombotic events and excessive tPA can lead to weak clots and accelerated fibrinolysis. TPA in plasma comes almost exclusively from endothelial cells[26], where it is stored in large quantities[27, 28]. If the vessel walls sustain a large injury, the ruptured endothelial cells can release enough tPA into the local plasma to trigger hyperfibrinolysis. Using our model, we show that parts of the vasculature with higher surface-area-to-volume ratios are more susceptible to the hypocoagulable state exhibited in ATC (Figure 3.1).

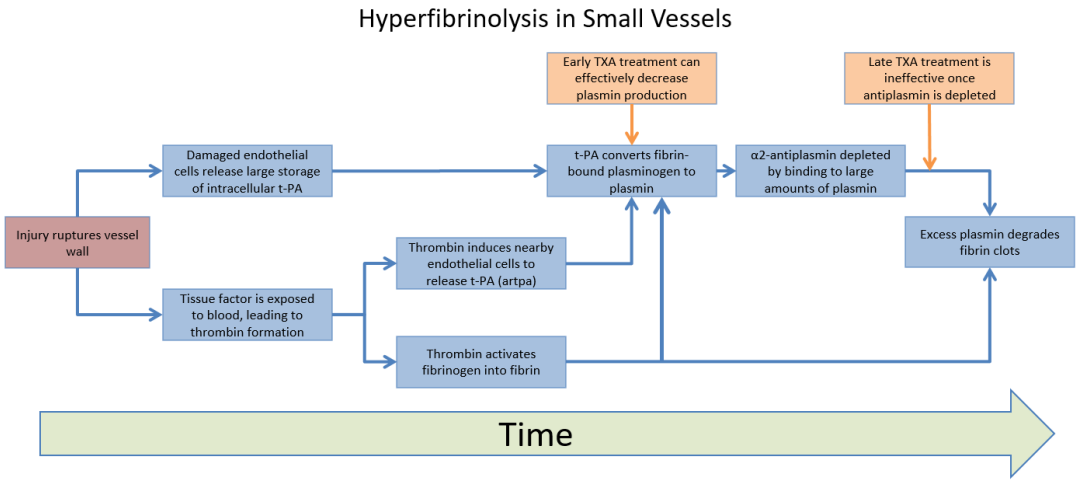

Figure 3.1: Simplified Sequence of Events Leading to Local Hyperfibrinolysis. After injury, the tPA contents of ruptured endothelial cells are released into the surrounding fluid. In small vessels, this release results in a disproportionately high concentration of tPA because of the high surface-area-to-volume ratio, leading to excessive plasmin formation. If antiplasmin becomes depleted from binding to large amounts of plasmin, the excess plasmin can break down the fibrin clot, resulting in hyperfibrinolysis. TXA can delay or prevent hyperfibrinolysis if provided early by decreasing the effective concentration of plasminogen, but has little effect if administered after antiplasmin has been depleted. Conditions can be exacerbated under conditions of shock, in which flow is impaired and/or the vessel is constricted.

In our study, we also examine how our model of ATC would respond to treatment by tranexamic acid, an anti-fibrinolytic used to reduce bleeding in surgery, trauma and menstruation. The use of TXA for trauma has been somewhat controversial as it appears that the treatment improves patient outlook if administered early but worsens outlook if administered after 3 hours post-admission[6]. Using excessive tPA to simulate the bleeding phenotypes of ATC, we were able to qualitatively reproduce the time-sensitive nature of the efficacy of TXA treatment reported in clincal trials[6].

3.1 Model (Methods)

Model (Methods)

Model Construction

We constructed a 2D rectangular domain (Figure 3.2) to represent our damaged blood vessel. The width of the domain is 10mm, and the height is varied between 10, 25, 50 and 100 μm, which covers the range of diameters in venules. The domain was discretized on a 50 x 25 grid, with a higher density of nodes near the bottom boundary. The left and right boundaries of the rectangle represent the inlet and outlet of the channel respectively. The top boundary is a non-reactive surface with a no-slip/no-flux boundary condition. The bottom is a reactive surface that includes the site of the injury. Details of the injury site model will be given later in this section. We model the vessel as a reaction-diffusion system. We used a diffusion coefficient of 5 x $10^{-7} cm^2/s$, as used in previous models[20, 29, 30].

We are interested in situations where the patient has sustained a massive amount of injury. Studies of patient microcirculation show that endothelial damage and shock severely impact flow in smaller vessels[31]. Thus, the simulations reported in the main body of this paper were undertaken with no convective flow (reaction and diffusion only) with periodic boundary conditions on the channel.

Model of Fibrin Formation and Degradation

The network of reactions used in our model includes the reactions for thrombin generation, fibrin formation and fibrin degradation in plasma. These reactions and their

associated rate constants are taken from models based on in vitro experimental results, and most of them can be found in previously published ODE models[15, 24, 11] and the full list of reactions can be found in the Appendix. To model fibrin deposition and polymerization, we do not allow fibrin species to convect or diffuse after formation. As a result, concentrations of fibrin near the injury site can exceed the initial concentration of fibrinogen.

tPA Release from Endothelial Cells

In addition to these reactions, we model tPA release from endothelial cells from three sources: (1) constitutive release, (2) acute release, and (3) intracellular release (labeled ctpa, artpa, ictpa in our model respectively). Constitutive release is the steady release from endothelial cells that establishes the basal concentration of tPA together with the basal concentration of plasminogen activator inhibitor-1 (PAI-1). While we expect constitutive production to vary based on region, constitutive release is slow enough that basal concentrations should not vary much region-to-region. The main contributors to the region-specific susceptability to hyperfibrinolysis are acute release and intracellular release. Acute release refers to the endothelial cell response of releasing tPA in the presence of thrombin, and intracellular release refers to intracellular tPA storage that can be dumped into the plasma instantaneously when cells rupture from injury[27]. Both of these sources are much more rapid than constitutive release, and the magnitude of the increase in tPA concentration scales inversely with vessel diameter. The rates of these reactions were calculated by fitting data from in vitro experiments performed by van den Eijnden-Schrauwen (1995)[27]. The initial values for tPA storage (maximum value of 150 pM/m^2) in endothelial cells were calculated based on in vivo estimates by Emeis (1992)[32], and we took the surface density of endothelial cells to be 1 x $10^5 cells/cm^2$[33].

PAI-1 Release from Platelets

There is also an "acute" anti-fibrinolytic response in endothelial cells that can scale with vessel diameter in a similar fashion. When exposed to inflammatory markers, endothelial cells can be induced to secrete PAI-1, which is the primary inhibitor to tPA. However, trauma-induced increases in PAI-1 secretion in endothelial cells over the basal rate is slower than the t-PA response as PAI-1 is not stored in significant amounts in endothelial cells compared to t-PA and therefore must be synthesized prior to release[34]. For this reason, we chose not to include this in our model. However, we do account for PAI-1 released from thrombin-activated platelets. To account for the potential effects of PAI-1 released from platelets, we used a value of 266 pM/m^2 for the amount of PAI-1 stored at the injury site. This approximated value was obtained using the maximum platelet concentration in a spatial model from Fogelson [20], and measured levels of PAI-1 release in thrombin stimulated platelets were taken from [35]. This allows us to obtain an upper bound on the amount of PAI-1 which can be released at the injury site. However, since the time resolution in the measurements was too coarse to obtain an accurate rate of release, we decided to use these reactions to gain an understanding of the potential of platelet PAI-1 instead of incorporating it into our main model. Details regarding tPA release and PAI-1 can be found in the Supplemental Information (SI).

Model of Vessel Wall and Injury Site

In our spatial simulations, we have modified the reactions from the ODE models by separating the fluid-phase reactions from the surface-phase reactions (see SI). It is important to separate the reactions because certain species such as tissue factor (TF) and thrombomodulin (TM) exist primarily on the surface of a blood vessel, thus the reactions associated with those surface species must take place on the surface. To accomplish this,

we took the platelet binding reactions from Kuharsky(2001)[36] to simulate the binding of coagulation factors to the injury surface. Those bound factors can then form the enzyme complexes at the injury site as a surface species. The rates of reactions between two surface species were adjusted from the original volumetric values in a similar way by using a constant boundary layer thickness of $1\mu m$ instead of a varying boundary layer thickness between 0 and $3\mu m$[36]. In addition to the factors bound to platelet binding sites (PBS), TF and TM were modeled as surface species that bind to fluid species to form enzyme complexes on the surface.

The bottom boundary is the most important part of our model. It represents the endothelial surface, including the site of injury. The entire surface constantly secretes tPA (constitutive release) into the plasma. Most of the bottom surface is anti-coagulant, in that the only reactive protein on it is thrombomodulin. The part that represents the injury site also contains tissue-factor, which is exposed to plasma upon injury, as well as PBS, the sites that coagulation factors bind to once platelets are activated and attached to the injury surface. We used an amount of tissue factor, 5 $pmol/m^2$, that leads to the same peak thrombin time as for the ODE simulations in Brummel-Orfeo-Mann (2012)[24]. The concentration of PBS was taken as the surface concentration of each binding site on a platelet[36], multiplied by the platelet concentration of 330 $fmol/m^2$. This concentration was fit to produce similar peak thrombin times as the ODE model[24]. A similar value is used in Kuharsky (2001)[36] for maximum activated platelet concentration on the subendothelium, which ranged from 220 to 660 $fmol/m^2$ depending on the height of the boundary layer. For our simulations, we assumed that the maximum number of PBS at the injury site is available from the start. In addition, the injury site also contains tPA to be released into the plasma via acute and intracellular release.

We took the injury site to be 20% (2 mm) of the length of the channel, starting 3mm into the channel. Along the bottom boundary, we allowed for reactions to occur between surface species, as well as between the surface and fluid species. We modeled this by introducing positive and negative fluxes in and out of the bottom boundary to simulate species being produced by and being bound to the endothelium. Additional details can be found in the SI.

Model for TXA Treatment

We simulated the effects of two methods of treatment: (1) Tranexamic Acid (TXA) and (2) Antiplasmin replenishment. TXA acts by binding to plasminogen, preventing plasminogen from binding to fibrin. Fibrin acts as a co-factor by providing a surface for t-PA to activate plasminogen, resulting in a greatly accelerated rate of plasmin generation compared to the solution phase reaction[37]. By inhibiting this binding, TXA effectively lowers the concentration of plasminogen in the system. We calculated that the standard dosage of TXA binds to roughly 90% of the plasminogen in the body based on pharmacokinetic properties presented in [38]. If administered intravenously, plasma concentrations can be maintained at this level for up to 5-6 hours[38]. Thus, to model TXA treatment, we instantaneously reduce the concentration of plasminogen to 10% of its current concentration in the system at various time points. To model antiplasmin replenishment treatment, we instantaneously increase the concentration of antiplasmin in the body by $1\mu M$ at various time points.

Computational Specifications

Our simulations were performed using the PETSc library (https://www.mcs.anl.gov/petsc/) on a 4 core 3.4 GHz Intel Core i7-3770k Processor. Each simulation took about an hour

to complete. Post-processing analysis was performed using MATLAB.

Results

Fibrinolysis Studies

We ran our simulations with and without intracellular tPA release, to show the potential impact of the release of the endothelial storage of tPA in triggering ATC. The magnitude of the impact depends on the extent of the injury. In our model, the simulations that included intracellular tPA release used injury intensities of 25%, 50%, 75% and 100%, referring to the amount of intracellular tPA released if that percentage of the cells at the injury site were injured. We also reduce the rate of constitutive release and acute release by the same amount to account for the reduced number of cells.

Effects of Vessel Size and Injury

We examined fibrin concentrations in vessels of differing diameters, in response to injury. In our simulations without intracellular tPA release (Figure 3.3a), we see that the size of the vessel has two effects on fibrin concentration. First, the peak fibrin concentration is lower in the smaller vessels. This is due to the larger control volumes in large vessels that allow for more fibrin to accumulate, as there is more fibrinogen which can diffuse toward the injury site, while the fibrin formed at the injury site cannot diffuse out as fibrin species are restricted from diffusion and convection in our model. Secondly, in the 25, 50 and 100 μm channels, the degradation is very slow, suggesting a very stable clot. However, in the 10 μm channel, we see that fibrin degradation starts to accelerate. The lower peak concentration and faster fibrinolysis suggest that smaller channels will be more susceptible to hyperfibrinolysis. When we incorporate a intracellular tPA

release from a 50% injury, fibrinolysis is sped up in all vessels but the effect is far more pronounced in the two smaller vessels(Figure 3.3b) in which the acceleration is very significant.

We find that the rate at which fibrinolysis increases is quite sensitive to the amount of tPA released from the injury site in the smaller vessels, while the larger vessels are much less sensitive to this parameter(Figure 3.4). This suggests that vessels of different size have a different threshold of tPA to trigger hyperfibrinolysis. Once the tPA threshold for hyperfibrinolysis has been exceeded, further tPA exposure can exacerbate the situation. We also find that if we include the release of PAI-1 from platelets in the model, it can delay the onset of hyperfibrinolysis, possibly increasing the tPA threshold, but has little potential to prevent it(Figure 3.5). This demonstrates that, although in theory a localized release of PAI-1 could offset the localized release of tPA, in reality the difference in magnitude of available tPA and PAI-1 make this possible only if the amount of tPA released during injury is close to its threshold.

The mechanism behind the acceleration of fibrinolysis in the smaller vessels is apparent when we examine the concentrations of plasmin and plasmin-antiplasmin(PAP) complex (Figure 3.6). The concentration of plasmin-antiplasmin approaches 1 μM (the initial concentration of antiplasmin) around the time that fibrinolysis starts to accelerate. This depletion of antiplasmin causes plasmin generation to go unregulated, which results in accelerated fibrin degradation. In addition, simulations with smaller injuries or longer channels have been performed (see SI) to ensure that the size of the injury compared to that of the channel did not affect the dynamics of the system. A smaller injury, as expected, delayed the onset of hyperfibrinolysis, but did not change the dynamics of the system. Thus, we performed our analysis on the larger injury to reduce computation

time and computation costs.

TXA and Antiplasmin Studies

We use the 25 μm vessel with 100% injury simulation as our surrogate for coagulopathic conditions because it allows us to apply the treatments at different stages of ATC in the 5000 second computation window. With that, we simulated the effectiveness of TXA treatment (Figure 3.7a). We found that if TXA is provided before fibrinolysis starts to accelerate, it can effectively re-stabilize the rate of fibrinolysis. However, the efficacy of TXA treatment falls off tremendously when treatment is provided after hyperfibrinolysis sets in. One discrepancy between these results and the clinical observations of the CRASH-2 studies[6] is that not only did TXA become ineffective when administered late, it also *increased* hemorrhaging. This is likely due to the unmodeled dynamics between TXA-bound plasminogen and urokinase-type plasminogen activator (uPA) in which TXA induces a shape change in plasminogen, making it a better substrate for uPA[39]. Since tPA activity normally dominates the effects of uPA in normal fibrinolysis, the net effect of inhibiting tPA far outweighs the impact of increasing uPA activity. However, if TXA is administered late, TXA not only fails to inhibit tPA as our results show, but its enhancing effects on uPA activity can explain the increased hemorrhaging observed in the clinical data. Since we know that antiplasmin depletion is the reason for accelerated fibrinolysis, we also simulated antiplasmin replenishment as a treatment to compare to TXA treatment (Figure 3.7b). We see that TXA treatment is more effective than antiplasmin treatment early, but antiplasmin treatment is more effective than TXA treatment at later treatment times. Since neither treatment could restore fibrin concentration (i.e.: could only slow down the rate of fibrin degradation), it is likely that fibrinogen replenishment is necessary in conjunction with these anti-fibrinolytic treatments.

Discussion

Our model provides a mechanistic explanation for ATC through excessive clot lysis rather than poor clot formation. The evidence for ATC through consumption of coagulation proteins and/or hemodilution derives from studies showing the correlation of trauma mortality to low levels of various coagulation factors, fibrinogen, high levels of d-dimer, and high levels of tissue-plasminogen activator (tPA)[40]. While low levels of coagulation factors and fibrinogen lead to poor clot formation, a depletion of fibrinogen and elevated levels of d-dimer can be indicative of successful fibrin formation and subsequent excessive fibrinolysis. However, one of the most evident deficiencies of the factor consumption and/or dilution hypothesis is the often simultaneous hypo and hypercoagulable profiles exhibited in severe trauma[41], since factor consumption and dilution are systemic phenomena. One of the studies that support the hyperfibrinolysis hypothesis found that the major indicator of trauma-induced coagulopathy was high circulating levels of tPA[10]. In this study, the authors added an additional 1 nM of extra tPA in their Thromboelastogram (TEG) assays in order to accentuate the difference in the clotting profiles of healthy and coagulopathic patients. Our results show that both the additional tPA needed to induce hyperfibrinolysis and the region-specific hemostatic tendencies in coagulopathy can be explained by differential susceptibility to hyperfibrinolysis from endothelial tPA release that is determined by vessel size and local injury intensity.

This mechanism allows for the excessive hemorrhaging brought on by accelerated fibrinolysis in some regions, while other regions can exhibit normal and possibly even excessive coagulation. This mechanism can also explain why hemorrhagic shock is often a predictor for ATC[7]. During hemorrhagic shock, the body redistributes bloodflow away from "luxury" organs via vasoconstriction to preserve function in the vital organs[42, 43].

This causes an even higher surface-area-to-volume ratio and impaired bloodflow in the portions of the vasculature, particularly in the microvasculature[31] around these "luxury organs", thus further exacerbating the region's susceptibility to hyperfibrinolysis. While elevated tPA expression is the trigger for the hyperfibrinolysis in our model, the root cause of the acceleration of fibrinolysis is the local depletion of antiplasmin. For this to occur, there are two requirements: (1) high local plasmin activation, which is facilitated by high concentrations of tPA in our model, and (2) a limited supply of antiplasmin (simulated in our model with a small control volume). However, hyperfibrinolysis could also be induced in vivo when hemorrhaging decreases the flow to these regions, thus effectively limiting the supply of proteins such as antiplasmin.

Our model focuses on the concentrations of blood proteins to find a mechanism for ATC. Thus, it does not capture some important dynamics that other models may include, such as the complex dynamic flow during coagulation[18, 19, 20], TAFI regulation[11], platelet dynamics[21], as well as complex mechanisms for fibrin degradation [22, 16]. Our model also does not capture the contribution of antiplasmin in stabilizing clots against fibrinolysis[44, 45, 46] which would further emphasize the pathological consequences of antiplasmin depletion. Spatial models are far more computationally costly than well-mixed models; because of this, the previously mentioned spatial models often use reduced-order reaction systems and choose to focus on other details. In contrast, we have chosen to focus on the reaction system to show the potential impact of the release of the endothelial storage of tPA in triggering ATC. Due to these limitations, we do not expect our model to be able to capture the exact behavior of in vivo hypocoagulation in ATC. Furthermore, we expect that the susceptibility to hyperfibrinolysis as well as the time of onset will be region dependent. In our model, we use the intracellular tPA from damaged endothelial cells as the source of extra plasmin activation required to trigger hyperfibrinolysis. At

the same time, there could be other contributing factors, such as increased inhibition of PAI-1 from increased levels of activated protein C [47], that could have impacts similar to that of the release of intracellular tPA in damaged endothelial cells.

Besides the region-specific coagulation profiles, our mechanistic explanation for ATC is consistent with other clinical observations as well. Hemorrhaging produced by this mechanism responds to TXA treatment in a similar time sensitive fashion as reported in clinical studies[6]. This phenomena cannot be explained by mechanisms of ATC associated with poor clot formation, as TXA does not improve the formation of clots, but instead it acts to slow down clot lysis[38]. Moreover, since the source of the increased fibrinolytic activity derives from the endothelium and not the plasma, our model is able to explain the limited effectiveness of transfusions to restore proper coagulation. Our results indicate that in ATC patients, the initial injury does not clot properly because extra tPA is introduced into the system from intracellular storage, as a direct result of injury. Even when plasma concentrations are restored through transfusion, the local tPA concentration at these injury sites will eventually deplete the antiplasmin in the local blood, leading to post-resuscitation hemorrhaging.

In addition, we were able to compare the effects of two different treatments for ATC. TXA treatment represents treatments that inhibit the zymogen, plasminogen, while antiplasmin treatments, such as the drug aprotinin (Tryasol)[48], inhibit the serine protease plasmin. Because these treatments use a different mechanism to inhibit fibrinolysis, the results can be different depending on the time at which the treatment is administered. While we cannot speak to the practicality or viability of antiplasmin as an anti-fibrinolytic treatment for trauma, having a mechanistic understanding of this disease should enable the exploration of options for treatment. [**?** **?**]. Figure **??**.

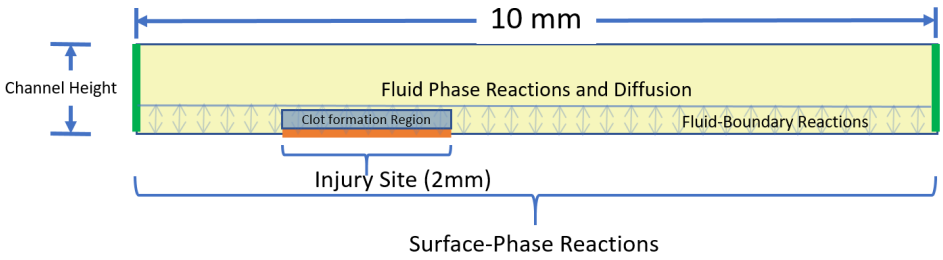

Figure 3.2: The computational model. The model is separated into two domains: the plasma containing fluid species that undergo fluid-phase reactions and diffusion, and the vessel surface with surface species that undergo surface-phase reactions in which surface species react with each other. The injury site is a 2 mm region on the surface containing additional surface species to represent the injury. There are also fluid-surface reactions at the interface which allow the two domains to exchange species. The results in this paper are measured in the clot formation region, which is a 2mm x 10μm area above the injury site. The height of the channel varies between 10, 25, 50 and 100 μm.

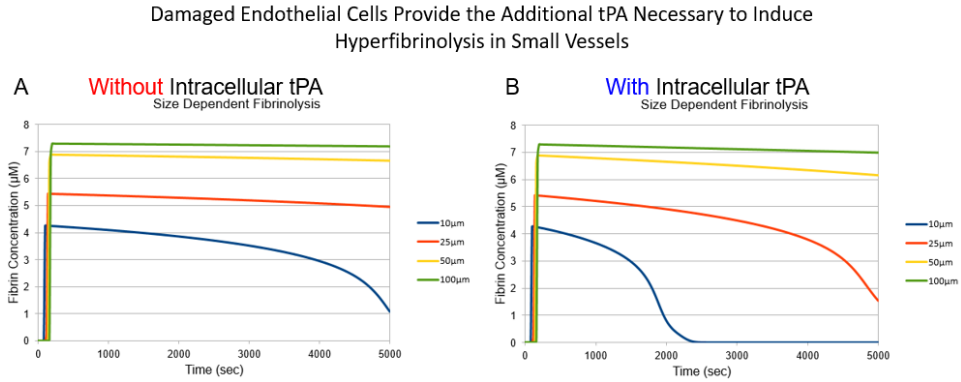

Figure 3.3: Simulations of Fibrin Concentrations in Various Sized Vessels in the (A) Absence and (B) Presence of intracellular T-PA release. (A) Fibrin concentrations are very stable for the 25, 50, 100 μm vessels under both conditions. In the case of the 10 μm simulation, fibrin degradation accelerates rapidly toward the end. (B) When intracellular tPA is added, there is little effect on fibrinolysis for the 50 and 100 μm vessels, but there is a very pronounced effect for the 10 and 25 μm vessels. Concentrations are calculated as average concentrations over the 2-D domain, 10 μm above the injury site.

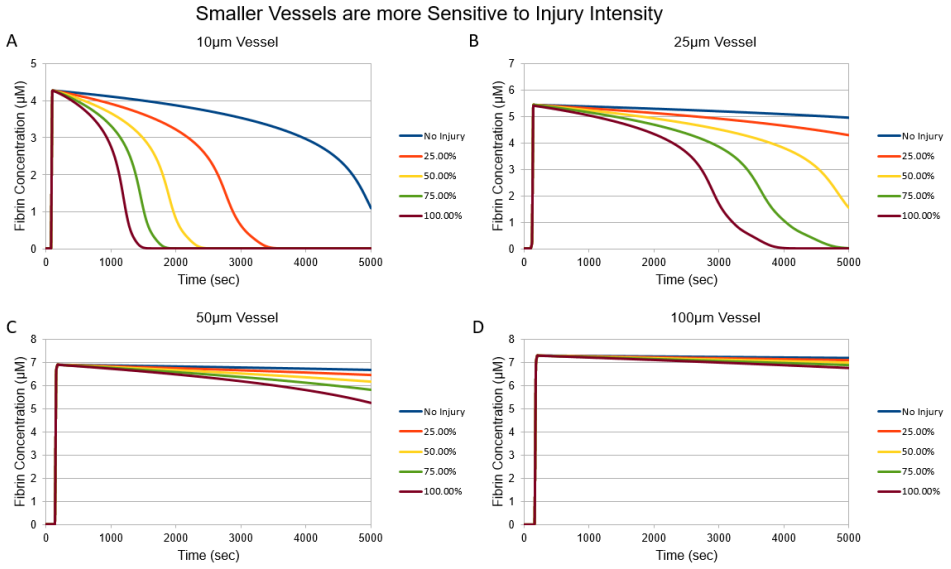

Figure 3.4: Simulations of the Effects of Injury Intensity on the Rate of Fibrinolysis on Vessels of Height: (A) 10 μm (B) 25 μm (C) 50 μm and (D) 100 μm. (A) In the 10 μm vessel, the rate of fibrinolysis is very sensitive to the level of injury, however it seems that hyperfibrinolysis has begun for all injury levels. (B) In the 25 μm vessel, we find that the range of tPA release in our model includes the critical point for which at low injury levels fibrinolysis may be stable, but at higher levels it can switch to becoming hyperfibrinolytic. In the larger vessels (C),(D), we find that the rate of fibrinolysis is not very sensitive to the level of injury, probably because the amount of tPA in the system has not reached the threshold necessary to induce hyperfibrinolysis. Concentrations are calculated as average concentrations over the 2-D domain, 10 μm above the injury site.

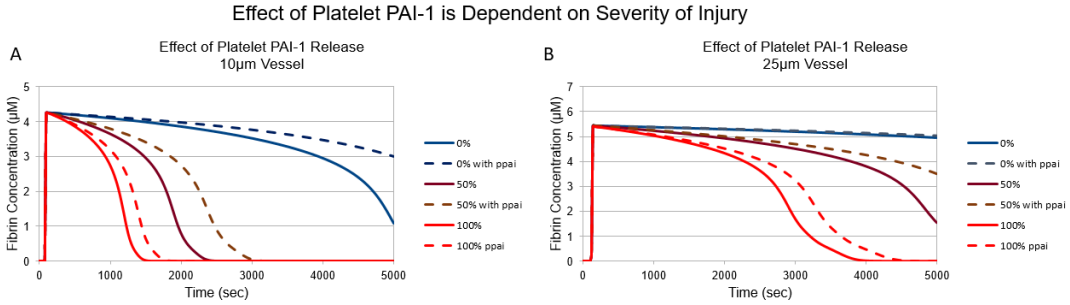

Figure 3.5: Simulations of Fibrinolysis in the Presence and Absence of Platelet PAI-1 Release in (A) 10 μm and (B) 25 μm Vessels. In both vessels we see that platelet PAI-1 release reduces the *effective* amount of tPA released from the injury. This delays the onset of hyperfibrinolysis but does not prevent it from occurring. Concentrations are calculated as average concentrations over the 2-D domain, 10 μm above the injury site.

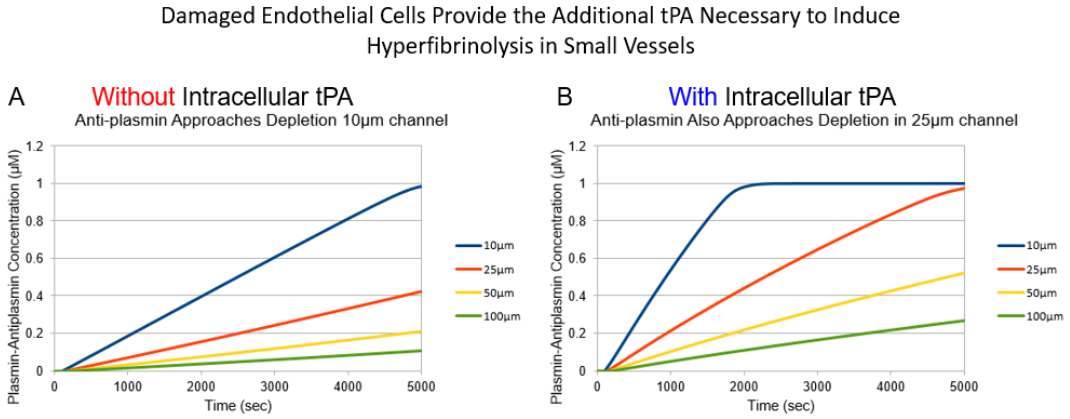

Figure 3.6: Simulations of Plasmin-antiplasmin (PAP) Complex Concentrations in the (A) Absence and (B) Presence of intracellular tPA release. (A) In the 10 μm vessel, the concentration of PAP approaches 1 μM, indicating that the antiplasmin is approaching depletion (initial concentration 1 μM). In contrast, in the 25, 50, 100 μm vessels, the PAP concentration increases far more slowly. (B) The presence of intracellular tPA release speeds up the rate at which PAP is formed in all vessels, and reaches saturation in the 10 μm vessel. The concentration of PAP approaches saturation in the 25 μm vessel and that's why we see fibrinolysis accelerate in Figure 3.3b. This explains why the additional tPA from intracellular release has a greater impact on fibrin degradation in the 10 μm and 25 μm simulations. Concentrations are calculated as average concentrations over the 2-D domain, 10 μm above the injury site.

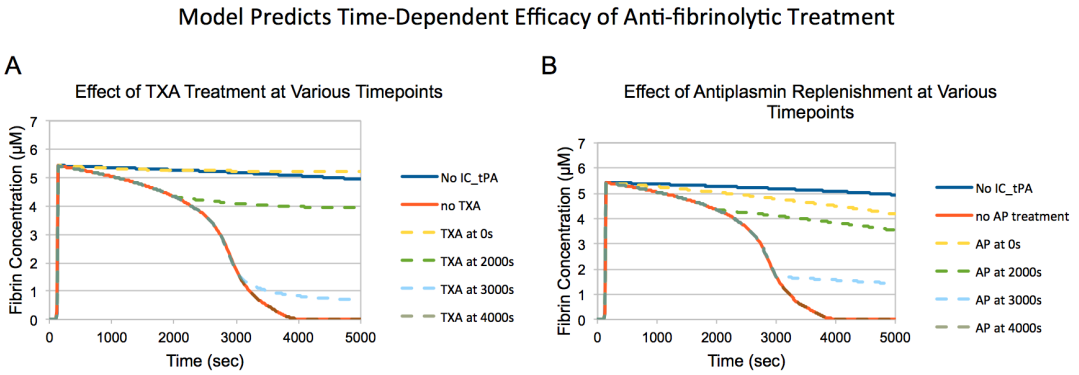

Figure 3.7: Simulations of Fibrinolysis Profiles when (A) TXA and (B) Antiplasmin (AP) Treatment is applied to a 25 μm vessel with 100% injury at Various Time Points. (A) Similar to reported clinical studies, the efficacy of TXA to slow down hyperfibrinolysis is very sensitive to the time at which it is administered. If applied early it is very effective, however if provided late, it can have little or no effect. (B) On the other hand, antiplasmin treatment is slightly less effective when given early but is better at slowing down the rate of fibrinolysis if provided later. However, neither have the ability to restore the lost clot strength once fibrin generation has ceased. Concentrations are calculated as average concentrations over the 2-D domain, 10 μm above the injury site.

Chapter 4

Modeling of the Behavior of Tranexamic Acid on Fibrinolysis

As previously mentioned, the mechanisms underlying ATC are not yet fully understood, making treatment difficult[3]. In this chapter, we focus on one treatment in particular, tranexamic acid (TXA). TXA has been found to be often effective[49, 50]. However, there are unknown circumstances in which the treatment has been reported to worsen the condition, with increased bleeding and mortality. A meta-analysis of the CRASH-2 study found that the relative risk of death due to bleeding in patients who received TXA compared to placebo was 0.68 for patients who arrived within 1 hour after injury, 0.79 for patients who arrived between 1 and 3 hours after injury, but 1.44 for patients who arrived more than 3 hours after injury[6, 51]. The risk of worsening the situation is one of the main reasons why many health care organizations are hesitant to incorporate TXA into their trauma protocol. Developing a mechanistic understanding of how TXA can produce such contrasting results is necessary for widespread adoption of the treatment.

Tranexamic acid is an antifibrinolytic amino acid derivative that prevents the binding

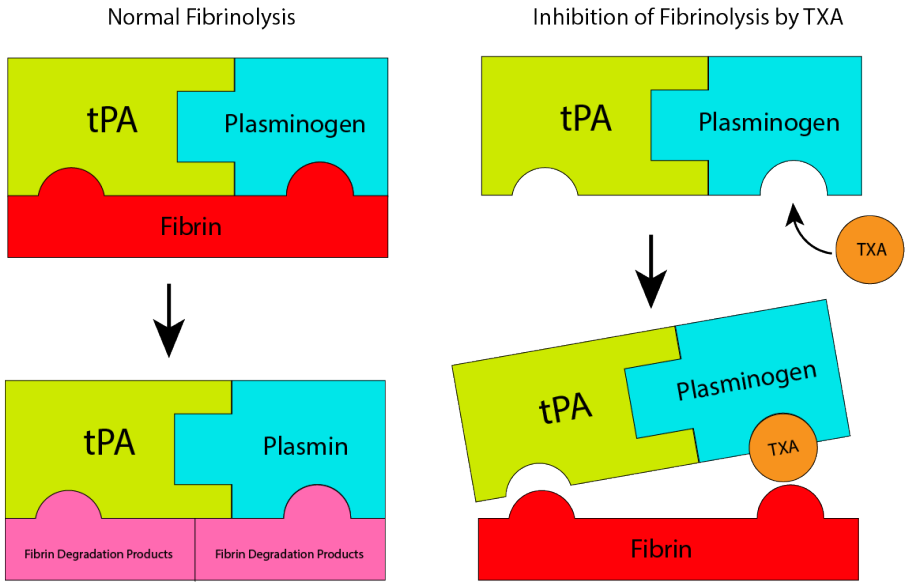

Figure 4.1: TXA interaction with plasminogen. Tranexamic Acid(TXA) inhibits fibrinolysis through its binding to plasminogen (Pg). This binding prevents plasminogen from binding to fibrin, which inhibits activation through tPA.

of plasmin(ogen) to fibrin. This binding inhibits fibrinolysis in two ways (Figure 4.1). First, it slows down tissue-plasminogen-activator(tPA) mediated conversion of plasminogen to plasmin, as fibrin acts as a substrate that increases the catalytic efficiency of the reaction 500-fold. Even after activation, TXA-bound plasmin cannot bind to fibrin, directly preventing the digestion of fibrin[52]. The mechanisms behind the anti-fibrinolytic properties of TXA are well understood, but the mechanism responsible for the possible increased bleeding and mortality have yet to be determined.

A possible explanation for the varying effectiveness of TXA treatment is the interaction between TXA and urokinase plasminogen activator (uPA or urokinase)[53]. Studies have shown that uPA levels are elevated in many instances in traumatic injury[54, 55], and since uPA-mediated plasmin activation occurs in solution, the inhibition of fibrin binding by TXA is inconsequential to this process. Furthermore, there is another binding site for TXA on plasminogen that induces a conformation change that speeds up plasmin

activation approximately 3-fold[56]. However this explanation is incomplete, as multiple studies have shown that despite the increase of plasmin generation, TXA still inhibits fibrinolysis in uPA-mediated systems[57, 58]. This suggests that other conditions must be met to change the behavior of TXA from anti-fibrinolytic to pro-fibrinolytic. To explore the possible conditions under which TXA can increase fibrinolysis through uPA-mediated plasmin generation, we constructed a differential equation based computational model. This model builds on previous ODE models[15, 24, 11, 59, 60] of the coagulation and fibrinolysis system, but focuses specifically on investigating the interaction between uPA and TXA, which are not present in these models.

We found that additional plasmin inhibitors such as α1-antitrypsin(A1AT) and α2-macroglobulin(A2M), two proteins not often associated with fibrinolysis, play a critical role in preventing TXA-induced hyperfibrinolysis (Figure 4.2. If the other plasmin inhibitors are depleted, α2-antiplasmin (AP or antiplasmin) is not sufficient in preventing fibrinolysis, and the presence of TXA acts to increase the rate of fibrinolysis.

Methods

Computational Model

In this paper we constructed an ordinary differential equation (ODE) model of the coagulation process. This includes reactions for thrombin generation, fibrin formation and fibrin degradation (Figure 4.2). Many of these reactions and their associated rate constants are taken from models based on in vitro experimental results, and most of them can be found in previously published ODE models[15, 24, 11, 59, 60].

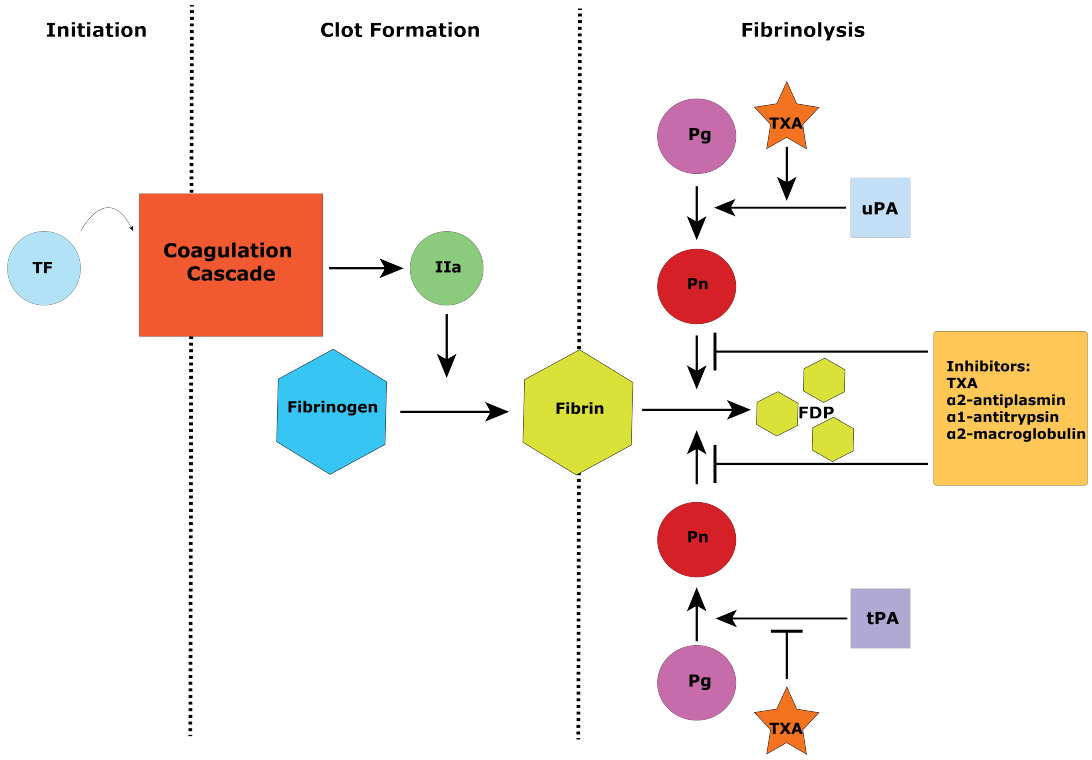

Figure 4.2: Simplified diagram of reaction network. This network diagram shows the important reactions in our model. Tissue factor (TF) initiates a chain of reactions in the coagulation cascade resulting in thrombin (IIa). Thrombin converts fibrinogen into fibrin, forming the clot. The clot is broken down by plasmin (Pn) which is activated from plasminogen (Pg) in one of two ways, by tissue-plasminogen activator (tPA) or urokinase-plasminogen activator (uPA). This diagram illustrates how tranexamic acid (TXA) has properties that both inhibit and promote fibrinolysis. The purpose of this paper is to explore which conditions cause the net effect to change from anti-fibrinolytic to pro-fibrinolytic. Additional abbreviation: Fibrin Degradation Productions (FDP).

Our model focuses on the interactions between TXA and fibrinolysis, so it includes a more detailed model of TXA-plasminogen binding (Figure 4.3). We model plasminogen with 2 binding sites for TXA (labeled x and y), resulting in 4 species of Pg, depending on whether TXA is bound to one or both of those sites (Pg, Pgx, Pgy, Pgxy). The x site controls the pro-fibrinolytic activity of TXA. If TXA is bound to this site ($K_d = 600\mu M$), then its activation rate via uPA is increased 3-fold. The y site controls the anti-fibrinolytic activity of TXA and has a much higher binding affinity ($K_d = 1.1\mu M$). This is the binding site that fibrin and plasmin inhibitors such as α2-antiplasmin bind to. If the y site

is occupied by TXA, it cannot bind to fibrin, which prevents it from being activated by tPA and prevents it from degrading fibrin even after being converted to plasmin. While tPA cannot activate the plasminogen species with its y site bound (Pgy, Pgxy), uPA can activate all of these species of plasminogen. Therefore, in uPA-mediated systems, TXA will increase the amount of plasmin generated[57, 56].

The reversibility of the TXA binding with plasmin(ogen) has an important consequence. It means that eventually TXA bound to the y site will be replaced by a irreversible plasmin inhibitor as long as there is some left in the system. This means that TXA is effective at inhibiting fibrinolysis only if there is a sufficient supply of plasmin inhibitors[60]. A complete description of the model, a complete list of reactions, rate constants and initial conditions for our model can be found in the Appendix. The full model can be found online at `https://github.com/taicheeze/coag_ode_julia`.

We initiated coagulation with 5 pM of tissue factor (TF), which is frequently used in other computational models[24]. We examined the rate of fibrinolysis initiated with 2.5 nM tPA or 5 nM uPA, and varied the amount of TXA in the system (0, 1, 3, 14, 54 and 3470 μM) to compare to experimental results to those of Longstaff 2019[58].

Results

TPA Mediated Fibrinolysis

The effects of TXA on tPA mediated fibrinolysis in our computational model behave as expected and are confirmed by results of previous empirical experiments(Figure 4.4)[61, 58, 57]. As more TXA was added to the system, fibrinolysis slowed down in a dose-

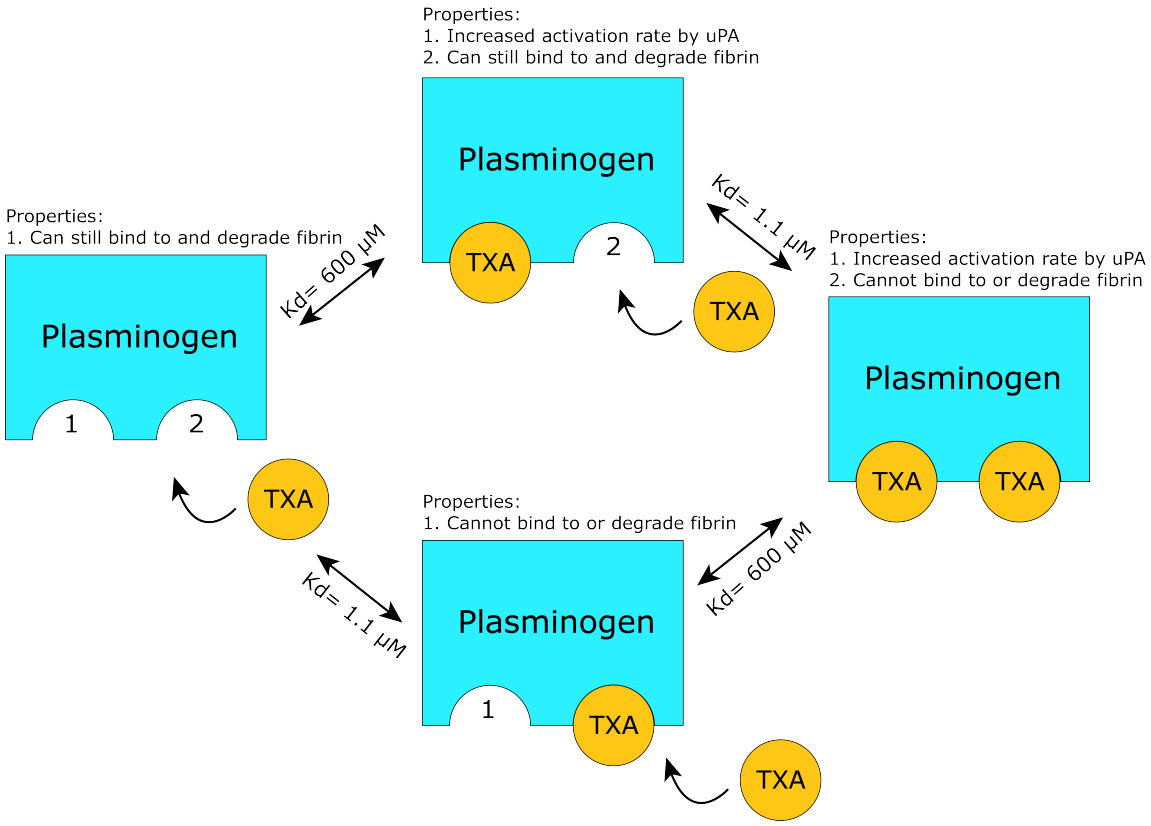

Figure 4.3: Diagram of different variants of TXA-bound plasminogen. Plasminogen has 2 binding sites that interact with TXA (labeled x and y in the model). One of the binding sites with $K_d = 600\mu M$ changes the conformation that speeds up activation by uPA. The other binding site with $K_d = 1.1\mu M$ prevents binding to fibrin, which prevents activation via tPA as well as fibrin degradation. UPA can activate all 4 of these variants, whereas tPA can activate only the variants with the second binding site free.

dependent manner. This behavior is consistent through different initial concentrations of plasmin inhibitors (not shown) as expected since the interactions between TXA and tPA are straightforward and well established. These results show that the bulk of the model, with the exception of the uPA pathway of fibrinolysis, is in agreement with empirical data.

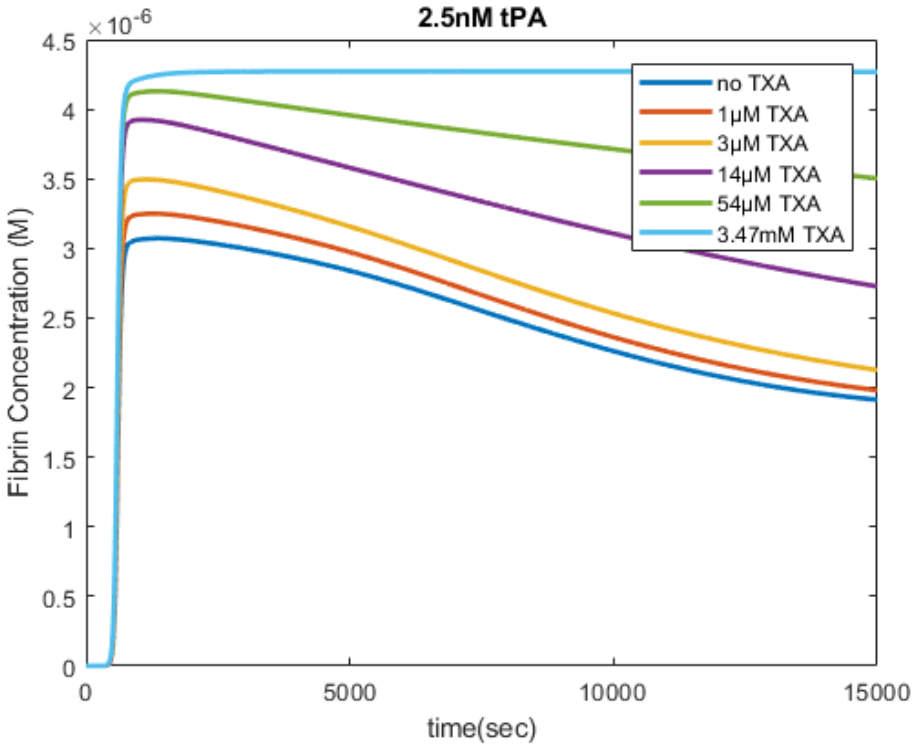

Figure 4.4: Effects of TXA on tPA mediated fibrinolysis. Modeling results show that Tranexamic Acid (TXA) affects tPA mediated fibrinolysis in a dose dependent fashion. As the concentration of TXA increases, the rate of fibrinolysis decreases. At the highest dose of TXA, fibrinolysis appears to be completely inhibited. These simulations are initiated with 5 pM tissue factor, and an initial tPA concentration of 2.5 nM.

UPA Mediated Fibrinolysis

The interactions between TXA and uPA are more complex. Overall, fibrinolysis with uPA is slower than with tPA, which can be for a variety of reasons. UPA activates plasmin in solution rather than on the fibrin surface, making it easier to inhibit by plasmin inhibitors. In our model, uPA is inhibited by protein C inhibitor (PCI) [62, 63] which is present in our system with a greater concentration than the inhibitors of tPA. We note that our model does not contain the many other reactions that can potentially consume A2M and A1AT, which affect uPA-activated plasmin more than tPA activated fibrin. Focusing on the plasmin inhibition role of these proteins, we simulated the effects of

consumption of these proteins by varying their initial concentrations. Under conditions simulated with high concentrations of plasmin inhibitors (Figure 4.5A), TXA behaves in an anti-fibrinolytic manner. Despite increasing the amount of plasmin in the system, the activated plasmin is quickly bound to TXA, preventing it from degrading fibrin. The TXA bound to the active plasmin is later replaced by one of the non-reversible plasmin inhibitors, which permanently inhibits it. Higher concentrations of TXA shift the equilibrium between TXA-bound plasmin and free plasmin, lowering the amount of free plasmin at any given time, resulting in quick inhibition by other plasmin inhibitors.

When α1-antitrypsin is removed from the system (Figure 4.5B), the behavior of the system remains mostly unchanged. The effects of A1AT are not obvious until both A1AT and A2M are removed. In this system, A1AT appears to play a role redundant to A2M except much weaker, due to its much slower binding to plasmin[64]. When A2M is removed from the system (Figure 4.5C), uPA mediated fibrinolysis becomes much more apparent. However, TXA retains its anti-fibrinolytic behavior, with a small change in behavior in the 10-100 μM range, which has also been shown experimentally[57].

However, once both A2M and A1AT are removed from the system(Figure 4.5D), the behavior of TXA flips. In this system, the only plasmin inhibitor left is antiplasmin. Since the ratio of plasminogen to antiplasmin is nominally 2:1, a large amount of plasmin activation can deplete antiplasmin. The presence of TXA increases the rate of plasmin activation, and since the binding between TXA and plasmin is reversible, antiplasmin will eventually deplete, and any remaining activated plasmin will rapidly degrade fibrin, resulting in hyperfibrinolysis.

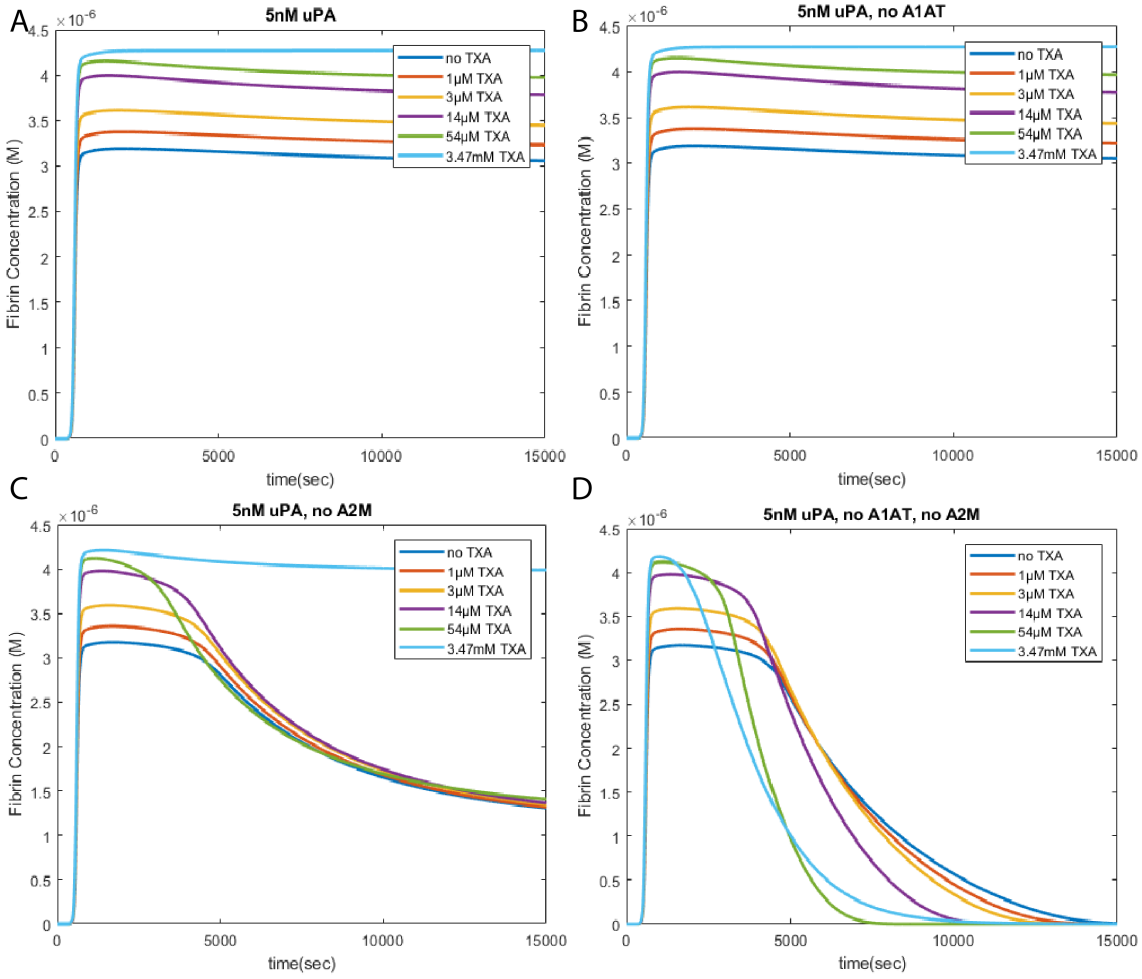

Figure 4.5: Effects of TXA on uPA mediated fibrinolysis. Modeling results reveal that the effect of TXA on uPA mediated fibrinolysis greatly depends on the presence or absence of plasmin inhibitors in the system. When A2M is in the system, with (A) or without (B) A1AT, fibrinolysis is inhibited and TXA behaves in an anti-fibrinolytic fashion. When A2M is removed from the system, but A1AT is still present (C), fibrinolysis can be observed. Under these circumstances, TXA exhibits anti-fibrinolytic behavior and acts to slow down fibrinolysis in a dose dependent manner. When both A2M and A1AT are removed from the system (D), TXA becomes pro-fibrinolytic, and speeds up the rate of fibrinolysis through increased plasmin generation and antiplasmin depletion. These simulations are initiated with 5 pM tissue factor, and an initial uPA concentration of 5 nM.

TPA and uPA Mediated Fibrinolysis

The behavior of TXA also depends on the balance between tPA and uPA in the system. In systems depleted of A1AT and A2M, TXA remains anti-fibrinolytic in the

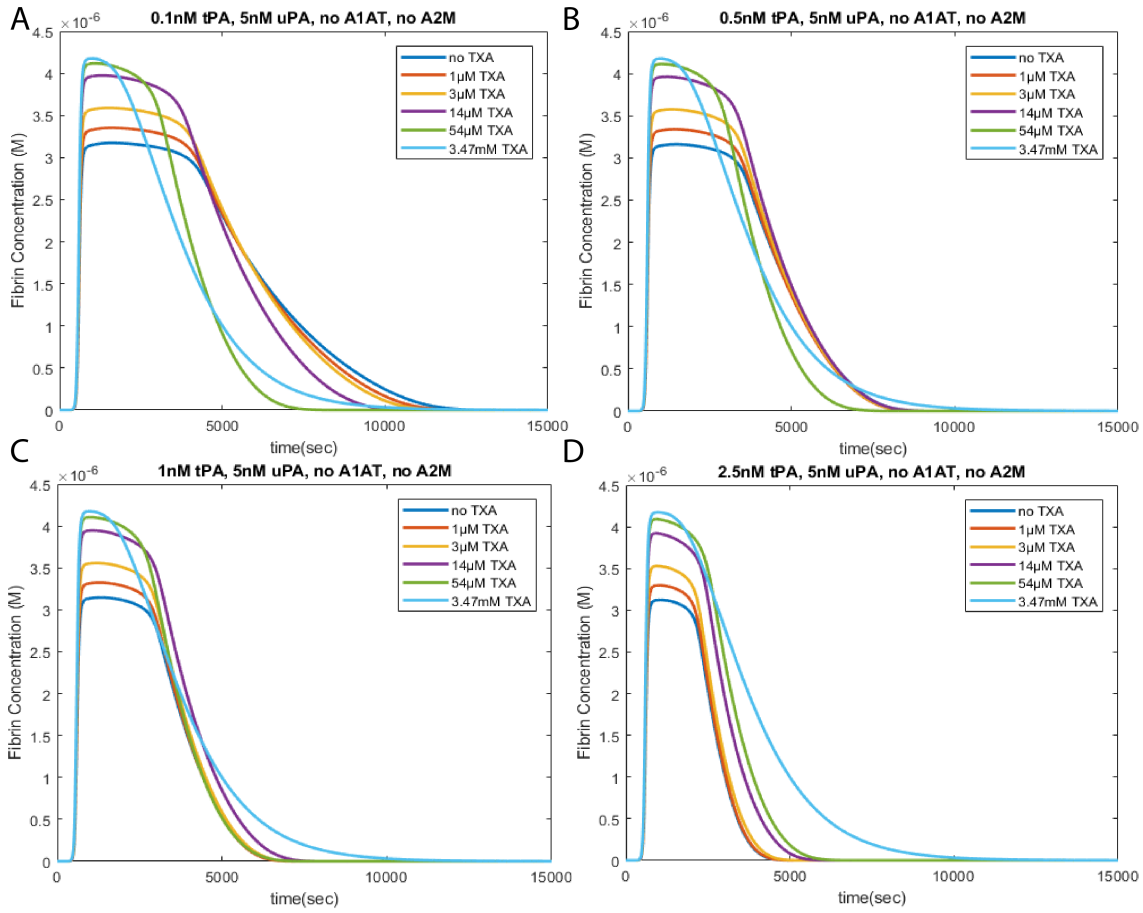

Figure 4.6: Effects of TXA on systems with both tPA and uPA. Modeling results show that the effect of TXA on systems with both tPA and uPA depend on the balance between the two pathways. The concentration of uPA is held constant at 5nM, as tPA is increased from 0.1nM to 2.5nM. When tPA is low compared tp uPA (A and B), TXA exhibits the pro-fibrinolytic behavior similar to figure 4.5D. This behavior shifts toward anti-fibrinolytic as tPA increases. At 1nM tPA (C), the hyperfibrinolysis occurs at similar times regardless of the concentration of TXA. At 2.5nM tPA (D), TXA is anti-fibrinolytic and acts to slow down hyperfibrinolysis. These simulations are initiated with 5 pM tissue factor.

tPA pathway, but becomes pro-fibrinolytic in the uPA pathway. By modulating the ratio of tPA to uPA, the overall effect of TXA can go from pro-fibrinolytic (Figure 4.6A and B), to no effect(Figure 4.6C) to anti-fibrinolytic(Figure 4.6D). We can see that across these concentrations of tPA, the curves for the highest TXA concentrations are more-or-less identical. This shows that at high concentrations of TXA, the tPA pathway is

completely inhibited.

Discussion

In this paper we have proposed a mechanistic explanation for the variance of outcomes in patients treated with TXA. In situations with elevated uPA and depletion of plasmin inhibitors such as A1AT and A2M, TXA can speed up fibrinolysis, leading to increased bleeding. Without A1AT and A2M, antiplasmin is quickly depleted and the generated plasmin rapidly breaks down any fibrin clots uninhibited. One possible mechanism for depletion of plasmin inhibitors during trauma may arise from the interactions between A1AT and A2M with activated Protein C (APC)[65]. Many studies have shown that high levels of protein C are correlated with trauma patients with worse outcomes[66, 47]. This is more likely to occur in patients that arrive late, as there is more time for the plasmin inhibitors to deplete. Furthermore, the likely concurrence of high tPA in the system during trauma can work in tandem to push a system toward hyperfibrinolysis[10]. Under these conditions, TXA increases the amount of plasmin produced by uPA in solution that rapidly consumes antiplasmin. Once antiplasmin has been reduced significantly, TXA loses its ability to prevent tPA-mediated fibrinolysis and any plasmin generated on fibrin surfaces will go uninhibited as A2M and A1AT cannot bind to fibrin-bound plasmin.

This model also provides an explanation for empirical studies that show how TXA can increase plasmin generation in uPA systems, but at the same time slow down fibrinolysis. This model shows that TXA binding to plasmin alone cannot prevent antiplasmin from depleting, because the binding between TXA and plasmin is reversible. Regardless of the amount of TXA in the system, free plasmin will always be present, but higher concentrations of TXA decreases the amount of free plasmin available. This free plasmin

will be consumed by plasmin inhibitors and shifts the equilibrium to generate more free plasmin. In healthy plasma, there is an ample supply of plasmin inhibitors, and TXA serves to lower the amount of free plasmin at any given time, leading to quick inhibition. However, if A2M and A1AT are depleted, TXA can act to speed up the rate of antiplasmin depletion because the concentration of plasminogen is approximately twice the concentration of antiplasmin. This leaves the remaining free plasmin free to break down fibrin unimpeded. Because of this, the presence of additional irreversible inhibitors is necessary in a functional fibrinolytic system.

Even in the absence of TXA, these additional inhibitors are necessary in healthy fibrinolysis. During an injury, tPA deposits in endothelial cells are quickly released in large amounts into the site of injury. During the time immediately after injury, plasmin activators greatly outnumber its inhibitors such as PAI-1 and can quickly activate large amounts of plasmin[60]. Without additional inhibitors, antiplasmin would quickly deplete, resulting in hyperfibrinolysis.

A mechanistic understanding of this phenomena has the potential to improve patient treatment significantly. Currently, the decision on whether to use TXA in treatment depends on whether the patient arrived before or after 3 hours post injury. Although this heuristic protocol can be helpful, it will undoubtedly lead to instances in which patients who can benefit from TXA treatment are not receiving it and patients who would suffer adversely from it will be given it. With an understanding of the conditions under which TXA helps or worsens a patientâĂŹs condition, we can identify patients that should receive TXA and ones that shouldnâĂŹt. In addition, TXA treatment can potentially be improved by using plasmin inhibitors in conjection with TXA to mitigate the risk of hyperfibrinolysis through the depletion of plasmin inhibitors.

Chapter 5

Conclusions and Future Directions

As we unfold the complexity of biology and human anatomy, the use of computational models will become increasingly more important for answering our questions. In this dissertation we showed two applications of computational models for answering questions in medicine. We were able to use these models to provide mechanistic explanations for many phenomena surrounding acute traumatic coagulopathy. We showed that the endothelial tPA released during injury can deplete the local supply of antiplasmin resulting in coagulopathy through hyperfibrinolysis. Furthermore, this mechanism of coagulopathy accounts for the region-specific hemostasis, the resistance to transfusion, and the time-dependent efficacy of TXA treatment. We also presented a mechanistic explanation for how TXA can be both anti-fibrinolytic or pro-fibrinolytic. We showed that the net effect of TXA on fibrinolysis depended on the concentration levels of plasmin inhibitors in the system.

The development of mechanistic understandings of this system has many potential clinical applications. This knowledge can be applied to improved trauma protocols and the development of new treatment options. Currently, coagulopathic patients are diagnosed using systemic clotting assays such as thromboelastography (TEG), prothrombin time

(PT) and partial thromboplastin time (PTT). These assays measure the overall clotting properties of blood which is usually taken away from the injury site. However, with a complex system like coagulation, there can be many different mechanisms for poor clotting, which can be remedied in different ways. With an established mechanistic understanding of the disease, we can shift toward assaying individual protein concentrations such as plasmin inhibitors to check for hyperfibrinolysis. Our work also shows that the local environment significantly impacts the clotting profile of the blood, so this work may influence the development of technologies to assess the conditions at the injury site. This work can also have potential impact on the development of new treatments for ATC. In this paper, we've identified the importance of plasmin inhibitors in preventing hyperfibrinolysis and how treatments such as TXA can be ineffective or even detrimental if given in to patients depleted of plasmin inhibitors. Knowing this, external plasmin inhibitors could potentially be used in conjunction with TXA to maintain the anti-fibrinolytic behavior of TXA.

Before these practical applications can be implemented, there still needs to be several iterations between computational models and empirical experiments. One important question to answer is how endothelial tPA concentrations vary in the body. Currently, the values used in the model come from experiments performed on human umbilical vein endothelial cells (HUVEC), so we don't know if endothelial cells have different concentrations of tPA in capillaries or arteries compared to veins. We also do not know how these concentrations vary in the cells of different regions of the body. Another important area of interest is how the body responds to fluid resuscitation. Transfusions are a necessary part of trauma therapy, but there are many complications that arise from it. These complications include hemodilution, inflammation and issues with restoring perfusion to organs[67, 68]. Once we understand what to expect when fluids are given we can model the injury site as it is receiving treatment allowing us to test different treatment options.

The models presented in this dissertation primarily focus on the chemical reactions in the coagulation network. To answer the questions for practical applications, more complex models may be necessary. Depending on the nature of the question, the model may require the integration of other mechanisms such as complex dynamic flow during coagulation[18, 19, 20], TAFI regulation[11], platelet dynamics[21], as well as complex mechanisms for fibrin degradation[22, 16], or even a full body model with organ function[69].

This dissertation presented two examples where computational models can be used to gain an mechanistic understanding of acute traumatic coagulopathy. Using our models, we were able to gain insight that would be near impossible to achieve on intuition alone. As our knowledge of biology and medicine grow, computational models will become increasingly necessary to leverage all of this information. Moving forward, we hope that this work will help illuminate the necessity of computational models and techniques in biological and medical research.

Appendix A

Model Details

A.1 Abbreviations

Roman numerals designate the coagulation factors, and if followed by a lower case letter a, it indicates the activated version. Exceptions to this are II(prothrombin), IIa(thrombin), mIIa(meizothrombin). Va3, Va5, Va53 represent partially proteolized forms of factor Va. A colon between species names indicate a complex formed between those species. Other abbreviations are as follows: AP, α_2-antiplasmin; APC, activated protein C; ATIII, antithrombin-III; FDP, fibrin degradation products; Fg, fibrinogen; FnI, fibrin I monomers; FnII, fibrin II monomers; FPA, fibrinopeptide A; FPB, fibrinopeptide B; HCF and LCA1, factor Va degradation products; PAI, plasminogen activator inhibitor-1; PC, protein C; Pg, plasminogen; Pn, plasmin; TF, tissue factor; TFPI, tissue factor pathway inhibitor; TM, thrombomodulin,;uPA, urokinase plasminogen activator; TXA, tranexamic acid; PCI, protein c inhibitor; a2mg, α2-macroglobulin; a1at, α1-antitrypsin. In the ODE model, Pgx, Pgy, Pgxy, Pnx, Pnz, Pnxz refer to plasminogen or plasmin bound to TXA at specific binding sites. APnc refers to antiplasmin without the c-terminal region. In the PDE model, there are 4 separate species for tPA (tissue-plasminogen ac-

tivator). stPA refers to the soluble molecule responsible for activating plasminogen, the other three are surface species that supply stPA into the system through 3 mechanisms: ctPA (constitutive release), artPA (acute release) and ictPA (intracellular release).

A.2 Model Structure

As mentioned in the main portion of the paper, we use a 2D rectangular domain to represent our damaged blood vessel. Since we are primarily interested in the chemical interactions between the injury site and the fluid, we believe that a 2-d rectangular domain can sufficiently capture these dynamics. The width of the domain is 10mm, and the height is varied between 10, 25, 50 and 100 μm. The domain was discretized on a 50 x 25 grid, with a higher density of nodes near the bottom boundary(Figure S1). Simulations were run on a finer mesh with twice as many elements along both x and y axes to test for mesh independence with indistinguishable results. The left and right boundaries of the rectangle represent the inlet and outlet of the channel respectively. The top boundary is a non-reactive surface with a no-slip/no-flux boundary condition. The bottom is a reactive surface that includes the site of the injury. There are additional surface nodes located on this surface which contain concentrations of surface species.

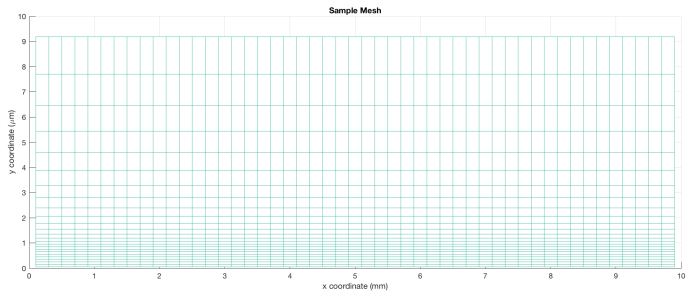

Figure S1: The Discretization Mesh. A 50 x 25 rectangular mesh is used to discretize our domain. The spacing of the x coordinates are uniform where as the y-coordinates are closer together near the bottom boundary. The y coordinates shown in this figure are specific to the 10 μm channel and they are scaled up for the larger channels.

We model the vessel as a reaction-diffusion system. We used a diffusion coefficient of 5 x $10^{-7} cm^2/s$, as used in previous models[20, 29, 30]. As mentioned in the main body of the paper, the results that were reported were from simulations with no convective flow (reaction and diffusion only) with periodic boundary conditions on the channel. However, simulations with flow were performed with similar results that do not change the conclusions presented in this paper.

We have modified the reactions from the ODE models by separating the fluid-phase reactions from the surface-phase reactions. It is important to separate the reactions because certain species such as tissue factor (TF) and thrombomodulin (TM) exist primarily on the surface of a blood vessel, thus the reactions associated with those surface species must take place on the surface. To accomplish this, we took the platelet binding reactions from Kuharsky(2001)[36] to simulate the binding of coagulation factors to the injury surface. Those bound factors can then form the enzyme complexes at the injury site as a surface species. The rates of reactions between two surface species were adjusted from the original volumetric values in a similar way by using a constant boundary layer thickness of $1\mu m$ instead of a varying boundary layer thickness between 0 and $3\mu m$[36]. In addition to the factors bound to platelet binding sites (PBS), TF and TM were modeled as surface species that bind to fluid species to form enzyme complexes on the surface.

As previously mentioned, the bottom boundary represents the endothelial surface, including the site of injury. The nodes of the surface contain surface species such as the endothelial t-PA which is secreted into the fluid domain. This release is represented as a boundary flux reaction in which a surface species (ctpa, artpa or ictpa) is converted to the fluid phase (stpa) so that it can activate plasminogen. Most of the bottom surface is anti-coagulant, in that the only reactive protein on it is thrombomodulin. The part that represents the injury site also contains tissue-factor, which is exposed to plasma

upon injury, as well as PBS, the sites that coagulation factors bind to once platelets are activated and attached to the injury surface. We used an amount of tissue factor, 5 $pmol/m^2$, that leads to the same peak thrombin time as for the ODE simulations in Brummel-Orfeo-Mann (2012)[24]. The concentration of PBS was taken as the surface concentration of each binding site on a platelet[36], multiplied by the platelet concentration of 330 $fmol/m^2$. This concentration was fit via parameter sweep to produce similar peak thrombin times as the ODE model[24]. A similar value is used in Kuharsky (2001)[36] for maximum activated platelet concentration on the subendothelium, which ranged from 220 to 660 $fmol/m^2$ depending on the height of the boundary layer. For our simulations, we assumed that the maximum number of PBS at the injury site is available from the start. In addition, the injury site also contains tPA to be released into the plasma via acute and intracellular release.

We took the injury site to be 20% (2 mm) of the length of the channel, starting 3mm into the channel. We chose this length for the injury site so that the injury was large enough to contain enough mesh elements to resolve the solution in the area without needing a finer mesh, but not so large that it became the driving mechanism behind the results. Simulations with different injury length were run, and lysis time decreased as injury length increased.

A.3 Kinetic Equations

The concentrations in our system are governed by the convection-diffusion-reaction equation. The general equation for a given fluid species i is:

$$\frac{\partial[C_i]}{\partial t} = \underbrace{-\nabla \cdot (\overrightarrow{u}[C_i])}_{\text{Convection}} + \underbrace{\nabla \cdot (D\nabla[C_i])}_{\text{Diffusion}} + \underbrace{R_i}_{\text{Reaction}}$$

In which C_i denotes the concentration of species i, $\overrightarrow{u}$ represents the fluid velocity vector, D represents the species diffusivity. The reactions, R_i, represent the sum of all reaction rates in which the species is a reactant or a product, the general form for these reactions can be found in the next section.

Since the results of this paper do not use flow, and we have constant diffusivity, the governing equation for a **fluid** species can be can be simplified to:

$$\frac{\partial[C_i]}{\partial t} = \underbrace{D\triangle[C_i]}_{\text{Diffusion}} + \underbrace{R_i}_{\text{Reaction}}$$

Furthermore, in our study, we assume that surface species do not diffuse as they are either bound to cells or platelet binding sites, the differential equation for **surface** species s, will only contain the reaction portion as such:

$$\frac{\partial[C_s]}{\partial t} = R_s$$

A.4 Calculating Reaction Rates

The reactions in this model can be reduced to three separate types: Fluid-Fluid, Surface-Surface and Surface-Fluid reactions. The following section details the process for calculating the reaction rates for each type of reaction.

A.5 Calculating Rates for Fluid-Fluid Reactions

Unless otherwise specified in Appendix B, reaction rates are calculated as standard mass action reactions. For example, given a reversible reaction between 3 Fluid Species,

F_1, F_2, and F_3, with a forward reaction rate constant k_1 and a backwards rate constant k_2:

$$F_1 + F_2 \rightleftharpoons F_3$$

We get the forward reaction rate $r_1 = k_1[F_1][F_2]$ and backwards reaction rate $r_2 = k_2[F_3]$. The rate of change of each species from reaction contribution (ignoring diffusion and convection), is the total rate of change after summing all of the production and depletion rates in which the species participates as either a reactant or a product.

A.6 Calculating Rates for Surface-Surface Reactions

With the exception of reaction 96, the Surface-Surface Reactions are also in the form of mass-action reactions. Many of our Surface-Surface Reactions were adapted from ODE models with only volumetric reactions. It is important to separate the reactions because certain species such as tissue factor (TF) and thrombomodulin (TM) exist primarily on the surface of a blood vessel, thus the reactions associated with those surface species must take place on the surface. To accomplish this, we took the platelet binding reactions from [36] to simulate the binding of coagulation factors to the injury surface. Those bound factors can then form the enzyme complexes at the injury site as a surface species. The rates of reactions between two surface species were adjusted from the original volumetric values in a similar way by using a constant boundary layer thickness of 1 μm instead of a varying boundary layer thickness between 0 and 3 μm [36]. In addition to the factors bound to platelet binding sites (PBS), TF and TM were modeled as surface species that bind to fluid species to form enzyme complexes on the surface.

We make this conversion by considering a boundary thickness, h, of $1\mu m$. Then for a species S_1, we can relate its volumetric concentration to its surface concentration, as well as the volumetric reaction rate to the surface reaction rate with the relationship:

$$[S_1]_v = \frac{[S_1]_s}{h}$$

$$r_v = \frac{r_s}{h}$$

Then, if we consider the original volumetric reaction between 3 Surface Species, S_1, S_2, and S_3, with a forward reaction rate constant k_3 and a backwards rate constant k_3:

$$S_1 + S_2 \rightleftharpoons S_3$$

We get the volumetric forward reaction rate $r_{v3} = k_3[S_1]_v[S_2]_v$ and volumetric backwards reaction rate $r_{v4} = k_4[S_3]_v$. If we convert the concentrations and rates to their surface counterparts, we get the following rates:

$$r_{s3} = \frac{k_3}{h}[S_1]_s[S_2]_s$$

$$r_{s4} = k_4[S_3]_s$$

The forward reaction can be re-written using a new constant, $\widetilde{k_3}$, with the relationship: $\widetilde{k_3} = \frac{k_3}{h}$ resulting in the forward reaction rate $r_{s3} = \widetilde{k_3}[S_1]_s[S_2]_s$. The values listed on Appendix C have already been adjusted using this conversion when appropriate. Then, similarly to the fluid reactions, the rate of change of the surface species is the sum of all of the production and depletion rates in which the species participates as either a reactant or a product.

A.7 Calculating Rates for Surface-Fluid Reactions

As mentioned in the article, changes to the fluid concentrations during a Surface-Fluid reaction are handled as a boundary flux. If we consider a reversible reaction between 2 Surface Species, S_3, S_4, and a Fluid Species F_3, with a forward reaction rate constant k_5 and a backwards rate constant k_6:

$$S_3 + F_3 \rightleftharpoons S_4$$

The surface reaction rates come out to $r_{s5} = k_5[S_3]_s[F_3]_v$ for the forward rate and $r_{s6} = k_6[S_4]_s$ for the backward rate. These are included when calculating the rate of change for the surface species as part of the set of reactions a surface species is involved with. We also use both of the right hand sides as the boundary fluxes $q_5 = -k_5[S_3]_s[F_3]_v$ (negative because it consumes the fluid species), and $q_6 = k_6[S_4]_s$, which are applied as boundary conditions on the surface on which the reaction occurs as:

$$\frac{\partial[F_1]}{\partial n} = \frac{1}{D}\sum_{i=1}^{L} q_i$$

Where n is the unit vector normal to the boundary (in our case it's always the y direction), D, is the diffusivity constant (we used 5 x$10^{-11} m^2/s$), L is the number of Surface-Fluid reactions that the fluid species is involved in and q_i are the individual boundary fluxes of each of those reactions.

A.8 Additional Information on Endothelial T-PA Release

The rates of these reactions were calculated by fitting data from in vitro experiments performed by van den Eijnden-Schrauwen (1995)[27]. The initial values for t-PA storage (maximum value of 150 pM m^{-2}) in endothelial cells were calculated based on in vivo estimates by Emeis (1992)[32], and we took the surface density of endothelial cells to be 1 x 105 cells cm^{-2}[33]. The parameter fitting for t-PA release was performed using the MATLAB Global Optimization toolbox, the fits are shown in Figure S2.

A.9 Additional Information on TXA Model

In order to model, we approximated the percentage of fibrinogen that would be bound after a dose of TXA. According to McCormack(2012)[38], the plasma concentration of TXA after a 1g dose was around 10 mg/L, this results to a molar concentration of approximately 60 μM. In the same paper, it is mentioned that only 3% of TXA in the plasma is bound to plasma proteins, of which almost all is attributed to plasminogen. This means that in healthy patients, approximately 1.8 μM of plasminogen was bound by TXA, which is 90% of our initial concentration. Thus, we model TXA infusion by instantaneously by removing 90% of the current plasminogen concentration at the time of activation.

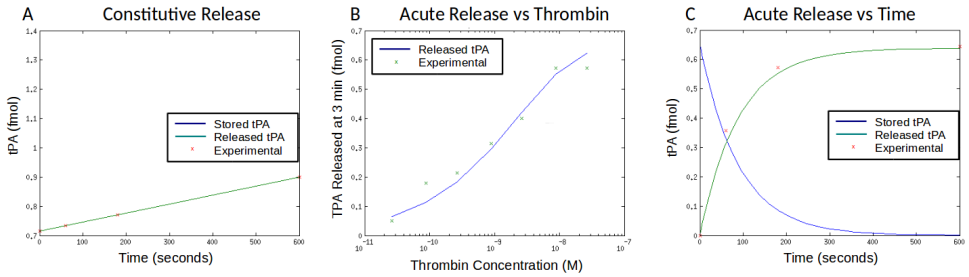

Figure S2: Fits for T-PA release. Data from van den Eijnden-Schrauwen (1995)[27] was used to fit the release rates for constitutive and acute release. Plots of the parameter fits for (A) constitutive release, the surface t-PA plot is not visible as it matches the top border of the plot, it is a constant line to show that the t-pa supply for constitutive release remains constant while releasing into the lumen at a linear rate. In order to capture the rate of acute release when stimulated by thrombin, parameters are fit to (B) the amount of t-PA released at 3 minutes when stimulated with varying concentrations of thrombin, as well as (C) time dependent measurements of t-PA release. Initial concentration measurements of intracellular release were based on amounts of t-PA measured from endothelial cell lysates.

A.10 Numerical Solver Information

The system of PDE's were solved using the PETSc PDE solver[70]. The problem is split into four parts using the method of operator splitting. At each time step, we solve surface reactions, volume reactions, convection (not applicable to this paper), and volume diffusion/boundary flux release independently, and then combine them afterwards. The reaction and diffusion steps are solved using Backward-Euler. The convection step (not used in this paper) is solved using Forward-Euler. The solver uses the PETSc **DMDA** library to construct the mesh and the **TS, SNES, KCP** libraries to solve the differential equations using finite difference methods. The minimum and maximum time steps provided to the **TS** solver were 1e-3 s and 1 s respectively. The absolute and relative tolerances are set to 1e-9, and 5e-3 respectively. The simulations performed in this paper were run on an Ubuntu system using a 4-core 3.4 GHz IntelCore i7-3770k Processor. Each simulation took about an hour to complete. Post-processing analysis was performed using MATLAB. For further details, the code is written in C and can be found at `https://github.com/taicheeze/coag_model`.

Appendix B

List of Fluid Reactions

#	Reaction	$k_{forward}(m^3/mol*s)$[1]	$k_{reverse}(1/s)$[1]
1	Xa+VII=>Xa+VIIa	1.30E+04	
2	IIa+VII=>IIa+VIIa	2.30E+01	
3	Xa+II=>Xa+IIa	7.5	
4	IIa+VIII=>IIa+VIIIa	2.00E+04	
5	VIIIa<=>VIIIa1L+VIIIa2	6.00E-03[3]	2.20E+01[4]
6	IIa+V=>IIa+Va	2.00E+04	
7	Xa+TFPI<=>XaTFPI	9.00E+02	3.60E-04
8	Xa+ATIII=>XaATIII	1.5	
9	mIIa+ATIII=>mIIaATIII	7.1	
10	IXa+ATIII=>IXaATIII	4.90E-01	
11	IIa+ATIII=>IIaATIII	7.1	
12	IIa+substrate=>IIa+fluorescence[2]	1	
13	IXa+X=>IXa+Xa	5.7	
14	mIIa+V=>mIIa+Va	3.00E+03	
15	APC+Va<=>APCVa	1.00E+05	7.00E-01
16	APCVa=>APC+Va5	1[3]	
17	APCVa=>APC+Va3	1.92E-01[3]	
18	APC+Va5<=>APCVa5	1.00E+05	7.00E-01
19	APC+Va3<=>APCVa3	1.00E+05	7.00E-01
20	APCVa5=>APC+Va53	1[3]	
21	APCVa3=>APC+Va53	1[3]	
22	Va3=>HCF+LCA1	2.80E-02[3]	
23	Va53=>HCF+LCA1	2.80E-02[3]	
24	APC+LCA1<=>APCLCA1	1.00E+05	7.00E-01
25	XI+IIa<=>IIaXI	1.00E+05	1.00E+01
26	IIaXI=>IIa+XIa	1.43[3]	
27	APC=>NULL	1.11E-03[3]	
28	Fg+IIa<=>Fg:IIa	1.00E+05	7.20E+02
29	Fg:IIa=>FnI+IIa+FPA	8.4E+01[3]	
30	FnI+IIa<=>FnI:IIa	1.00E+05	7.50E+02
31	FnI:IIa=>FnII+IIa+FPB	7.4[3]	
32	2FnI<=>FnI_2	1.00E+03	6.40E-02
33	FnI_2+IIa<=>FnI_2:IIa	1.00E+05	7.50E+02
34	FnI_2:IIa=>$FnII_2$+IIa+2FPB	4.90E+01[3]	
35	FnII+IIa<=>FnII:IIa	1.00E+05	1.00E+03
36	FnI_2:IIa+ATIII=>FnI2:IIa:ATIII	1.60E+01	
37	FnI:IIa+ATIII=>FnI:IIa:ATIII	1.60E+01	

[1]Default units unless specified.

[2]Reaction originally included to compare to experimental results detecting thrombin concentration via fluorescent antibodies.

This reaction is not relevant to this particular paper and was disabled by setting initial concentration of substrate species to zero.

[3]Units of s^{-1}.

[4]Units of $m^3/mol*s$.

List of Fluid Reactions cont.

#	Reaction	$k_{forward}(m^3/mol*s)^1$	$k_{reverse}(1/s)^1$
38	FnII:IIa+ATIII=>FnII:IIa:ATIII	1.00E+01	
39	Pn+AP=>Pn:AP	4.00E+02	
40	FnII=>FDP[4]	—	
41	$FnII_2$=>2FDP[4]	—	
42	stPA+PAI=>stPA:PAI	4.50E+02	
43	Pg=>Pn [5]	—	
44	FnI=>FDP[4]	—	
45	FnI2=>2FDP[4]	—	
46	PAI+APC=>PAI:APC	1.80E+02	

Reactions and rate constants for reactions 1-27, except 12, come from Brummel-Ziedins(2012)[24]. Reactions and rate constants for reactions 28-38 come from analysis on Ref. [71] done by Mitrophanov (2014)[11]. Reaction 39 and the corresponding rate constant come from Schneider (2004)[72] using the value for anti-plasmin binding in the presence of fibrin. Reactions and reaction rates for reactions 40, 41, 44, 45 come from Kim (2007)[73]. Reaction 42 and the corresponding rate constant come from Hekman (1988)[74]. Reaction 43 and the corresponding kinetic constants come from Mitrophanov (2014)[11] which were adaptations from Horrevoets (1996)[75].

[1]Default units unless specified.

[3]Units of s^{-1}.

[4]The reaction rate of fibrin degradation is determined using the following Michaelis-Menten formulation:

[0]

$$r_n = \frac{K_1[Pn][Fibrin]}{K_2+[Fibrin]}$$

[0]where r_n is the reaction rate associated with reaction n, [Fibrin] is the fibrin species in reaction n, $K_1 = 0.47s^-1$,
$K_2 = 2.1x10^{-3}mol/m^3$

[5]The reaction rate of plasminogen activation is determined using the steady-state template model described in Horrevoets (1996)[75]:

[0]

$$r_{43} = \frac{K_3[stPA][Pg][F]/(K_4+[F])}{[Pg]+K_5(K_6+[F])/(K_4+[F])}$$

[0]where $[F] = [FnII]+2[FnII_2]$, $K_3 = 9.0x10^{-2}s^{-1}$, $K_4 = 7.7x10^{-5}mol/m^3$, $K_5 = 4.1x10^{-4}mol/m^3$, $K_6 = 3.0x10^{-4}mol/m^3$

Appendix C

List of Surface Reactions

#	Reaction	$k_{forward}(m^3/mol*s)^1$	$k_{reverse}(1/s)^1$
1	TF+VII<=>TF:VII	3.20E+03	3.10E-03
2	TF+VIIa<=>TFV:IIa	2.30E+04	3.10E-03
3	TF:VIIa+VII=>TF:VIIa+VIIa	4.40E+02	
4	TF:VIIa+X<=>TF:VIIa:X	2.50E+04	1.05E+00
5	TF:VIIa:X=>TF:VIIa:Xa	6.00[3]	
6	TF:VIIa+Xa<=>TF:VIIa:Xa	2.20E+04	1.90E+01
7	TF:VIIa+IX<=>TF:VIIa:IX	1.00E+04	2.40E+00
8	TF:VIIa:IX=>TF:VIIa+IXa	1.8000e+00[3]	
9	TF:VIIa:Xa+TFPI<=>TF:VIIa:Xa:TFPI	3.20E+05	1.10E-04
10	TF:VIIa+Xa:TFPI=>TFVIIa:Xa:TFPI	5.00E+04	
11	TF:VIIa+ATIII=>TFVIIa:ATIII	2.30E-01	
12	IX+P9<=>IX:P9	1.00E+04	2.50E-02
13	IXa+P9<=>IXa:P9	1.00E+04	2.50E-02
14	IXa+P9s<=>IXa:P9s	1.00E+04	2.50E-02
15	X+P10<=>X:P10	1.00E+04	2.50E-02
16	Xa+P10<=>Xa:P10	1.00E+04	2.50E-02
17	V+P5<=>V:P5	5.70E+04	1.70E-01
18	Va+P5<=>Va:P5	5.70E-03	1.70E-01
19	VIII+P8<=>VIII:P8	5.00E+04	1.70E-01
20	VIIIa+P8<=>VIII:aP8	5.00E+04	1.70E-01
21	II+P2<=>II:P2	1.00E+04	5.90E+00
22	IIa+P2<=>IIa:P2	1.00E+04	5.90E+00
23	V:P5+Xa:P10<=>V:P5:Xa:P10	1.00E+10[2]	1.00E+00
24	VP:5:Xa:P10=>Va:P5+XaP10	4.60E-02[3]	
25	V:P5+IIaP2=>Va:P5+IIa:P2	2.00E+09[2]	
26	VIII:P8+Xa:P10<=>VIII:P8:Xa:P10	5.10E+09[2]	1.00E+00
27	VIII:P8:Xa:P10=>VIIIa:P8+Xa:P10	2.30E-02[3]	
28	IIa:P2+VIII:P8=>IIa:P2+VIIIa:P8	2.00E+09[2]	
29	IXa:P9:VIIIa:P8+X:P10<=>IXa:P9:VIIIa:P8:X:P10	1.00E+10[2]	1.00E-03
30	IXa:P9:VIIIa:P8:X:P10=>IXa:P9:VIIIa:P8+Xa:P10	8.20E+00[3]	
31	IXa:P9s:VIIIa:P8+X:P10<=>IXa:P9s:VIIIa:P8:X:P10	1.00E+10[2]	1.00E-03
32	IXa:P9s:VIIIa:P8:X:P10=>IXa:P9s:VIIIa:P8+Xa:P10	8.20E+00[3]	
33	Xa:P10:Va:P5+II:P2<=>Xa:P10:Va:P5:II:P2	1.00E+10[2]	1.03E+02
34	Xa:P10:Va:P5:II:P2=>Xa:P10:Va:P5+mIIa:P2	6.35E+01[3]	
35	IXa:P9+VIIIa:P8<=>IXa:P9:VIIIa:P8	1.00E+09[2]	5.00E-03
36	IXa:P9s+VIIIa:P8<=>IXa:P9s:VIIIa:P8	1.00E+09[2]	5.00E-03
37	Xa:P10+Va:P5<=>Xa:P10:Va:P5	4.00E+10[2]	2.00E-01
38	mIIa:P2+Xa:P10:Va:P5=>IIa:P2+Xa:P10:Va:P5	2.30E+10[2]	
39	VIIIa:P8<=>VIIIa1L:P8+VIIIa2	6.00E-03[3]	2.20E+01[4]
40	IXa:P9:VIIIa:P8:X:P10=>VIIIa1L:P8+VIIIa2+IXa:P9+X:P10	1.00E-03[3]	
41	IXa:P9s:VIIIa:P8:X:P10=>VIIIa1L:P8+VIIIa2+IXa:P9s+X:P10	1.00E-03[3]	
42	IXa:P9:VIIIa:P8=>VIIIa1L:P8+VIIIa2+IXa:P9	1.00E-03[3]	
43	IXa:P9s:VIIIa:P8=>VIIIa1L:P8+VIIIa2+IXa:P9s	1.00E-03[3]	
44	VIIIa1L:P8=>VIIIa1L+P8	1.70e-01[3]	
45	mIIa+P2<=>mIIa:P2	1.00E+04	5.90E+00
46	X+IXa:P9:VIIIa:P8<=>IXa:P9:VIIIa:P8:X	1.00E+05	1.00E-03
47	IXa:P9:VIIIa:P8:X=>Xa+IXa:P9:VIIIa:P8	8.20E+00[3]	
48	X+IXa:P9s:VIIIa:P8<=>IXa:P9s:VIIIa:P8:X	1.00E+05	1.00E-03

[1]Default units unless specified.
[2]Units of $m^2/mol*s$
[3]Units of s^{-1}.
[4]Units of $m^3/mol*s$

List of Surface Reactions cont.

#	Reaction	$k_{forward}(m^3/mol*s)$[1]	$k_{reverse}(1/s)$[1]
49	IXa:P9s:VIIIa:P8:X=>Xa+IXa:P9s:VIIIa:P8	8.20E+00[3]	
50	II+Xa:P10:Va:P5<=>Xa:P10:Va:P5:II	1.00E+05	1.03E+02
51	Xa:P10:VaP5:II=>mIIa+Xa:P10:Va:P5	6.35E+01[3]	
52	Xa:P10:Va:P5+mIIa=>Xa:P10:Va:P5+IIa	2.30E+05	
53	Xa:P10+VII=>Xa:P10+VIIa	1.30E+04	
54	IIa:P2+VII=>IIa:P2+VIIa	2.30E+01	
55	Xa:P10+II=>Xa:P10+IIa	7.50E+00	
56	Xa:P10+II:P2=>Xa:P10+IIa:P2	7.50E+05[2]	
57	Xa+II:P2=>Xa+IIa:P2	7.50E+00	
58	IIa+VIII:P8=>IIa+VIIIa:P8	2.00E+04	
59	IIa:P2+VIII=>IIa:P2+VIIIa	2.00E+04	
60	IIa+V:P5=>IIa+Va:P5	2.00E+04	
61	IIa:P2+V=>IIa:P2+Va	2.00E+04	
62	IIa:P2+substrate=>IIa:P2+fluorescence	1.00E+00	
63	Va3+P5<=>Va3:P5	5.70E-03	1.70E-01
64	Va5+P5<=>Va5:P5	5.70E-03	1.70E-01
65	Va53+P5<=>Va53:P5	5.70E-03	1.70E-01
66	Xa:P10+Va3:P5<=>Xa:P10:Va3:P5	4.00E+10[2]	1.50E-01
67	Xa:P10+Va5:P5<=>Xa:P10:Va5:P5	4.00E+10[2]	1.50E-01
68	Xa:P10:Va5:P5+II:P2<=>Xa:P10:Va5:P5:II:P2	1.00E+10[2]	1.03E+02
69	Xa:P10:Va5:P5:II:P2=>Xa:P10:Va5:P5+mIIa:P2	1.03E+01[3]	
70	Xa:P10:Va3:P5+II:P2<=>Xa:P10:Va3:P5:II:P2	1.00E+10	1.03E+02
71	Xa:P10:Va3:P5:II:P2=>Xa:P10:Va3:P5+mIIa:P2	1.03E+01[3]	
72	mIIa:P2+Xa:P10:Va5:P5=>IIa:P2+Xa:P10:Va5:P5	4.60E+09[2]	
73	mIIa:P2+Xa:P10:Va3:P5=>IIa:P2+Xa:P10:Va3:P5	4.60E+09[2]	
74	Xa:P10:Va3:P5=>HCF+LCA1+Xa:P10	3.50E-03[3]	
75	Xa:P10:Va3:P5:II:P2=>HCF+LCA1+Xa:P10+II:P2	3.50E-03[3]	
76	Xa:P10+Va53:P5<=>Xa:P10:Va53:P5	4.00E+10[2]	1.50E-01
77	Xa:P10:Va53:P5+II:P2<=>Xa:P10:Va53:P5:II:P2	1.00E+10[2]	1.03E+02
78	Xa:P10:Va53:P5:II:P2=>Xa:P10:Va53:P5+mIIa:P2	1.03E+01[3]	
79	mIIa:P2+Xa:P10:Va53:P5=>IIa:P2+Xa:P10:Va53:P5	4.60E+09[2]	
80	Xa:P10:Va53:P5=>HCF+LCA1+Xa:P10	3.50E-03[3]	
81	Xa:P10:Va53:P5:II:P2=>HCF+LCA1+Xa:P10+II:P2	3.50E-03[3]	
82	II:P2+Va:P5<=>II:P2:Va:5	1.00E+10[2]	7.00E+01
83	Xa:P10:Va5:P5+APC=>Xa:P10:Va53:P5+APC	4.05E+03	
84	TM+IIa<=>TM:IIa	1.00E+05	3.30E-01
85	TM:IIa+PC<=>TM:IIa:PC	1.00E+05	1.00E+02
86	TM:IIa:PC=>TM:IIa+APC	4.10E-01[3]	
87	TM:IIa+ATIII=>IIa:ATIII+TM	7.10E+00	
88	TM:IIa+APC<=>TM:IIa:APC	1.00E+05	1.00E+02
89	TM+mIIa<=>TM:mIIa	1.00E+05	3.30E-01
90	TM:mIIa+PC<=>TM:mIIa:PC	1.00E+05	1.00E+02
91	TM:mIIa:PC=>TM:mIIa+APC	4.10E-01[3]	
92	TM:mIIa+ATIII=>mIIa:ATIII+TM	7.10E+00	

[1]Default units unless specified.
[2]Units of $m^2/mol*s$
[3]Units of s^{-1}.

List of Surface Reactions cont.

#	Reaction	$k_{forward}(m^3/mol*s)^1$	$k_{reverse}(1/s)^1$
93	ctPA=>stPA	2.21E-05[3]	
94	NULL<=>ctPA[4]	1.57E-14	1.93E-04
95	NULL<=>artPA [4]	1.02E-15	3.47E-04
96	artPA=>stPA[5]	—	
97	ictPA=>stPA	0.0116[3]	

Rate constants associated with the binding of fluid species to PBS are from Kuharsky *et al.*[36]). The remainder of the rate constants are from Brummel-Ziedens *et al.*[24]), with the exception of the rate constants for reactions 62, 93-98. The rate constants for 93-98 were fit to data in van den Eijnden-Schrauwen (1995)[27].

[1]Default units unless specified.

[2]Units of $m^2/mol*s$

[3]Units of s^{-1}.

[4]These reactions represent the synthesis/degradation of constitutive (ctPA) and acute release tPA (artPA), the forward reaction rate

is the rate of production in units of $m^3/mol*s$, these rates were fit from data from van den Eijnden-Schrauwen (1995)[27], if intra-cellular tPA is turned on, these

rates are halved to simulate half of the cells rupturing from injury (rates away from the injury have little effect).

[5]The thrombin-induced release rate of artPA was fit to the data from van den Eijnden-Schrauwen (1995)[27], with the form:

$$sr_{96} = k_1[artPA][IIa]^2$$

where $k_1 = 4.06(mol/m^3)^{-0.5} * s^{-1}$

Appendix D

List of Reactions in ODE model

#	Reaction	$k_{forward}(m^3/M*s)$[1]	$k_{reverse}(1/s)$[1]
1	TF + VII ⇌ TF_VII	3.20E+06	3.10E-03
2	TF + VIIa ⇌ TF_VIIa	2.30E+07	3.10E-03
3	TF_VIIa + VII → TF_VIIa + VIIa	4.40E+05[2]	
4	Xa + VII → Xa + VIIa	1.30E+07	
5	Iia + VII → Iia + VIIa	2.30E+04	
6	TF_VIIa + X ⇌ TF_VIIa_X	2.50E+07	1.05E+00
7	TF_VIIa_X → TF_VIIa_Xa	6.00E+00[2]	
8	TF_VIIa + Xa ⇌ TF_VIIa_Xa	2.20E+07	1.90E+01
9	TF_VIIa + IX ⇌ TF_VIIa_IX	1.00E+07	2.40E+00
10	TF_VIIa_IX → TF_VIIa + Ixa	1.80E+00[2]	
11	Xa + II → Xa + Iia	7.50E+03	
12	Iia + VIII → Iia + VIIIa	2.00E+07	
13	VIIIa + IXa ⇌ VIIIa_IXa	1.00E+07	5.00E-03
14	VIIIa_IXa + X ⇌ VIIIa_IXa_X	1.00E+08	1.00E-03
15	VIIIa_IXa_X → VIIIa_IXa + Xa	8.20E+00[2]	
16	VIIIa ⇌ VIIIlca1 + VIIIa2	6.00E-03	2.20E+04[3]
17	VIIIa_IXa_X → VIIIlca1 +VIIIa2 + X + IXa	1.00E-03[2]	
18	VIIIa_IXa → VIIIlca1 +VIIIa2 + IXa	1.00E-03[2]	
19	IIa + V → IIa + Va	2.00E+07	
20	Va + Xa ⇌ Xa_Va	4.00E+08	2.00E-01
21	Xa_Va + II ⇌ Xa_Va_II	1.00E+08	1.03E+02
22	Xa_Va_II → Xa_Va + mIIa	6.35E+01[2]	
23	mIIa + Xa_Va → IIa + Xa_Va	2.30E+08	
24	Xa + TFPI ⇌ Xa_TFPI	9.00E+05	3.60E-04
25	TF_VIIa_Xa + TFPI ⇌ TF_VIIa_Xa_TFPI	3.20E+08	1.10E-04
26	TF_VIIa+Xa_TFPI → TF_VIIa_Xa_TFPI	5.00E+07	
27	Xa + ATIII → Xa_ATIII	4.20E+03	
28	mIIa + ATIII → mIIa_ATIII	7.10E+03	
29	IXa + ATIII → IXa_ATIII	4.90E+02	
30	IIa + ATIII → IIa_ATIII	1.60E+04	
31	TF_VIIa + ATIII → TF_VIIa_ATIII	2.30E+02	
32	TM + IIa ⇌ TM_IIa	1.00E+08	3.30E-01
33	TM_IIa + PC ⇌ TM_IIa_PC	1.00E+08	1.00E+02
34	TM_IIa_PC → TM_IIa + APC	4.10E-01	
35	TM_IIa + ATIII → TM_IIa_ATIII	7.10E+03	
36	APC + Va ⇌ APC_Va	1.00E+08	7.00E-01
37	APC_Va → APC + Va5	1.00E+00[2]	
38	APC_Va → APC +Va3	1.92E-01[2]	
39	APC + Va5 ⇌ APC_Va5	1.00E+08	7.00E-01
40	APC + Va5 ⇌ APC_Va5	1.00E+08	7.00E-01
41	APC_Va3 → APC + Va53	1.00E+00[2]	
42	APC_Va5 → APC + Va53	1.92E-01[2]	

[1]Default units unless specified.
[2]Units of s^{-1}.
[3]Units of $1/M*s$.

List of Reactions in ODE model cont.

#	Reaction	$k_{forward}(m^3/M*s)$[1]	$k_{reverse}(1/s)$[1]
43	Va3 → HCF + LCA1	2.80E-02[2]	
44	Va53 → HCF + LCA1	2.80E-02[2]	
45	APC+LCA1 ⇌ APC_LCA1	1.00E+08	7.00E-01
46	TM_IIa + APC ⇌ TM_IIa_APC	1.00E+08	1.00E+02
47	Va5 + Xa ⇌ Xa_Va5	1.50E+08	1.50E-01
48	Va3 + Xa ⇌ Xa_Va3	1.50E+08	1.50E-01
49	Xa_Va5 + II ⇌ Xa_Va5_II	1.00E+08	1.03E+02
50	Xa_Va5_II → Xa_Va5 + mIIa	1.03E+01[2]	
51	Xa_Va3 + II ⇌ Xa_Va3_II	1.00E+08	1.03E+02
52	Xa_Va3_II → Xa_Va3 + mIIa	1.03E+01[2]	
53	mIIa + Xa_Va5 → IIa + Xa_Va5	4.60E+07	
54	mIIa + Xa_Va3 → IIa + Xa_Va3	4.60E+07	
55	Xa_Va3 → Xa + HCF + LCA1	3.50E-03[2]	
56	Xa_Va3_II → Xa + II + HCF + LCA1	3.50E-03[2]	
57	IXa + X → IXa + Xa	5.70E+03	
58	mIIa + V → mIIa + Va	3.00E+06	
59	TM + mIIa ⇌ TM_mIIa	1.00E+08	3.30E-01
60	TM_mIIa + PC ⇌ TM_mIIa_PC	1.00E+08	1.00E+02
61	TM_mIIa_PC → TM_mIIa + APC	4.10E-01[2]	
62	TM_mIIa + ATIII → TM_mIIa_ATIII	7.10E+03	
63	Va53 + Xa ⇌ Xa_Va53	1.50E+08	1.50E-01
64	Xa_Va53 + II ⇌ Xa_Va53_II	1.00E+08	1.03E+02
65	Xa_Va53_II → Xa_Va53 + mIIa	1.03E+01[2]	
66	mIIa + Xa_Va53 → IIa + Xa_Va53	4.60E+07	
67	Xa_Va53 → Xa + HCF + LCA1	3.50E-03[2]	
68	Xa_Va53_II → Xa + II + HCF + LCA1	3.50E-03[2]	
69	II + Va ⇌ II_Va	1.00E+08	7.00E+01
70	Xa_Va5 + APC → Xa_Va53 + APC	4.05E+06	
71	APC → NULL	1.10E-03[2]	
72	Fg + IIa ⇌ Fg_IIa	1.00E+08	7.20E+02
73	Fg_IIa → FnI + IIa + FPA	8.40E+01[2]	
74	FnI + IIa ⇌ FnI_IIa	1.00E+08	7.50E+02
75	FnI_IIa → FnII + IIa + FPB	7.40E+00[2]	
76	2FnI ⇌ FnI2	1.00E+06	6.40E-02
77	FnI2 + IIa ⇌ FnI2_IIa	1.00E+08	7.50E+02
78	FnI2_IIa ⇌ FnII2 + IIa + 2FPB	4.90E+01[2]	
79	FnII + IIa ⇌ FnII_IIa	1.00E+08	1.00E+03
80	FnI2_IIa + ATIII → FnI2_IIa_ATIII	1.60E+04	
81	FnI_IIa + ATIII → FnI_IIa_ATIII	1.60E+04	
82	FnII_IIa + ATIII → FnII_IIa_ATIII	1.00E+04	
83	Pn + AP → Pn_AP	3.00E+06	
84	stPA + FnII ⇌ stPA_FnII	1.00E+04	5.80E-03

[1]Default units unless specified.
[2]Units of s^{-1}.

List of Reactions in ODE model cont.

#	Reaction	$k_{forward}(m^3/M*s)$[1]	$k_{reverse}(1/s)$[1]
85	stPA + FnII2 $\rightleftharpoons$ stPA_FnII2	1.00E+04	5.80E-03
86	stPA + PAI $\rightarrow$ stPA_PAI	4.50E+05	
87	Pn_FnII $\rightarrow$ Pn + FDP	3.13E-01[2]	
88	Pn_FnII2 $\rightarrow$ Pn + 2FDP	3.13E-01[2]	
89	APC + PAI $\rightarrow$ APC_PAI	1.80E+05	
90	Pg $\rightarrow$ Pn (uPA)[3]		
91	Pgx $\rightarrow$ Pgx (uPA)[3]		
92	TXA + Pg $\rightleftharpoons$ Pgx	1.00E+08	6.00E+04
93	PAI + uPA $\rightarrow$ uPA_PAI	7.90E+06	
94	Pn + TXA $\rightleftharpoons$ Pnx	1.00E+08	6.00E+04
95	Pg + FnII $\rightleftharpoons$ Pg_FnII	1.00E+05	2.20E-01
96	Pg + FnII2 $\rightleftharpoons$ Pg_FnII2	1.00E+05	2.20E-01
97	Pg_FnII $\rightarrow$ Pn_FnII (tPA)[4]		
98	Pg_FnII2 $\rightarrow$ Pn_FnII2 (tPA)[4]		

[1]Default units unless specified.

[2]Units of s^{-1}.

[3]The reaction rate of uPA-mediated plasmin activation is determined using the following Michaelis-Menten formulation:

$$r_n = \frac{K_1[uPA][Pg]}{K_2+[Pg]}$$

where r_n is the reaction rate associated with reaction n, [Pg] is the plasminogen species in reaction n, $K_1 = 0.73s^{-1}$,

for Pg, Pgy and $K_1 = 1.85s^{-1}$ for Pgx and Pgxy, $K_2 = 2.5x10^{-5}M$

[4]The reaction rate of tPA-mediated plasmin activation is determined using the following Michaelis-Menten formulation:

$$r_n = \frac{K_3[tPA][Pg]}{K_4+[Pg]}$$

where r_n is the reaction rate associated with reaction n, [Pg] is the plasminogen species in reaction n, $K_1 = 0.11s^{-1}$,

$K_4 = 1.9x10^{-7}M$

List of Reactions in ODE model cont.

#	Reaction	$k_{forward}(m^3/M*s)^1$	$k_{reverse}(1/s)^1$
99	Pn + FnII ⇌ Pn_FnII	1.00E+05	5.00E-02
100	Pn + FnII2 ⇌ Pn_FnII2	1.00E+05	5.00E-02
101	Pgx + TXA ⇌ Pgxy	1.00E+08	1.10E+02
102	Pg + TXA ⇌ Pgy	1.00E+08	1.10E+02
103	Pgy + TXA ⇌ Pgxy	1.00E+08	6.00E+04
104	Pgx + FnII2 ⇌ Pgx_FnII2	1.00E+05	2.20E+00
105	Pnx + FnII2 ⇌ Pnx_FnII2	1.00E+05	5.00E-02
106	Pgxy → Pnxz (uPA)[3]		
107	Pn + TXA ⇌ Pnz	1.00E+08	4.50E+03
108	Pnx + TXA ⇌ Pnxz	1.00E+08	4.50E+03
109	Pnz + TXA ⇌ Pnxz	1.00E+08	6.00E+04
110	Pgy → Pn + TXA (uPA)[3]		
111	Pgx → Pnx (tPA)[4]		
112	Pnx_FnII2 → Pnx + 2FDP	3.13E-01[2]	
113	Pnx + AP → Pn_AP	7.50E+04	
114	Pnz + AP → Pn_AP	7.50E+04	
115	Pnxz + AP → Pn_AP	7.50E+04	
116	Pn_FnII2 + AP → Pn_AP + FnII2	7.50E+04	
117	Pnx_FnII2 + AP → Pn_AP +FnII2	7.50E+04	
118	Pg_FnII2 → Pn_FnII2 (uPA)[3]		
119	Pgx_FnII2 → Pnx_FnII2 (uPA)[3]		
120	uPA + PCI → NULL	2.00E+03	
121	Pn + APnc → Pn_AP	7.50E+04	
122	Pnx + APnc → Pn_AP	1.88E+03	
123	Pnx_FnII2 + APnc → Pn_AP	1.88E+03	
124	Pn + A2M → Pn_A2M	1.11E+05	
125	Pnx + A2M → Pn_A2M	1.11E+05	
126	Pnz + A2M → Pn_A2M	1.11E+05	
127	Pnxz + A2M → Pn_A2M	1.11E+05	
128	Pn + A1AT → Pn_A1AT	4.00E+02	
129	Pnx + A1AT → Pn_A1AT	4.00E+02	
130	Pnz + A1AT → Pn_A1AT	4.00E+02	
131	Pnxz + A1AT → Pn_A1AT	4.00E+02	

Reactions and rate constants for reactions 1-71 come from[24]. Reactions and rate constants for reactions 72-82 come from analysis on Ref.[71] done by Ref.[11]. Reaction 83 and the corresponding rate constant come from Ref.[72]. Reactions and reaction rates for reactions 84-85, 95-96, 99-100, 104-105 come from Ref.[59]. Reaction 86 and the corresponding rate constant come from Ref.[74]. Reactions and reaction rates for reactions 87, 88, 112 come from Ref.[73]. Reaction 89 and the corresponding rate constant come from Ref.[76]. Reactions and reaction rates for reactions 91, 93, 106, 110, 118-119 come from Ref.[56]. Reactions and reaction rates for reactions 92, 94, 101-103, 107-109 come from Ref.[77]. Reaction 97, 98, 111 and the cor-

responding kinetic constants come from Ref.[25]. Reactions and reaction rates for reactions 112-117, 121-123 come from Ref.[78]. Reaction 120 and the corresponding rate constant come from Ref.[62]. Reactions and reaction rates for reactions 124-131 come from Ref.[64].

[1]Default units unless specified.

[2]Units of s^{-1}.

[3]The reaction rate of uPA-mediated plasmin activation is determined using the following Michaelis-Menten formulation:

$$r_n = \frac{K_1[uPA][Pg]}{K_2+[Pg]}$$

where r_n is the reaction rate associated with reaction n, [Pg] is the plasminogen species in reaction n, $K_1 = 0.73s^{-1}$,

for Pg, Pgy and $K_1 = 1.85s^{-1}$ for Pgx and Pgxy, $K_2 = 2.5x10^{-5}M$

[4]The reaction rate of tPA-mediated plasmin activation is determined using the following Michaelis-Menten formulation:

$$r_n = \frac{K_3[tPA][Pg]}{K_4+[Pg]}$$

where r_n is the reaction rate associated with reaction n, [Pg] is the plasminogen species in reaction n, $K_1 = 0.11s^{-1}$,

$K_4 = 1.9x10^{-7}M$

Appendix E

Initial Values

Initial Values in PDE model

Species[1]	Type	Initial Value[2]	Reference
VII	Fluid	1.00E-05	[24]
VIIa	Fluid	1.00E-07	[24]
IX	Fluid	9.00E-05	[24]
TFPI	Fluid	2.50E-06	[24]
II	Fluid	1.40E-03	[24]
V	Fluid	2.00E-05	[24]
ATIII	Fluid	3.40E-03	[24]
VIII	Fluid	7.00E-07	[24]
X	Fluid	1.60E-04	[24]
PC	Fluid	6.50E-05	[24]
Fg	Fluid	9.00E-03	[79]
Pg	Fluid	2.00E-03	[80]
AP	Fluid	1.00E-03	[80]
PAI[3]	Fluid	4.00E-08/1.20E-06	[26]
stPA[3]	Fluid	1.00E-08/2.00E-09	[26]
TF[4]	Surface	5.00E-12	[24]
TM	Surface	2.50E-10	[24]
P2[4]	Surface	6.60e-10	[36]
P5[4]	Surface	9.90E-10	[36]
P8[4]	Surface	1.49E-10	[36]
P9[4]	Surface	8.25E-11	[36]
P9s[4]	Surface	8.25E-11	[36]
P10[4]	Surface	8.91E-10	[36]

Initial Values in PDE model cont.

Species[1]	Type	Initial Value[2]	Reference
ctPA[5]	Surface	7.00E-11/3.5E-11	[27]
artPA[5]	Surface	2.97E-11/1.49E-11	[27]
ictPA[5]	Surface	0/7.50E-11	[27]

[1]If unlisted, initial value is zero

[2]Units are mol/m^3 for fluid species and mol/m^2 for surface species

[3]The first value corresponds to the low PAI-1 phenotype, the second value corresponds to the high PAI-1 phenotype as given in

ref [26], the difference on fibrinolysis at an injury site were not significant so only results from the low PAI-1 phenotype were used in

the paper.

[4]The initial concentrations of these species are as listed at the injury site and 0 everywhere else on the bottom surface. Binding sites

per platelet numbers were used from ref [36], final concentrations assumed an activated platelet concentration of 330 $fmol/m^2$

[5]The first value corresponds to the initial concentration at the injury site without intra-cellular tPA release and the concentration in

the rest of the channel. The second value corresponds to the initial concentration at the injury site when intra-cellular tPA release is

turned on.

Initial Values in ODE model

Species[1]	Initial Value[2]	Reference
VII	1.00E-08	[24]
TF	5.00E-12	[24]
VIIa	1.00E-10	[24]
X	1.60E-07	[24]
IX	9.00E-08	[24]
II	1.60E-06	[24]
VIII	7.00E-10	[24]
V	2.00E-08	[24]
TFPI	2.50E-09	[24]
ATIII	3.40E-06	[24]
TM	1.00E-09	[24]
PC	6.50E-08	[24]
FG	9.00E-06	[79]
AP	6.50E-07	[80]
stPA	varies	[26]
PAI	5.00E-11	[26]
Pg	2.00E-06	[80]
uPA	0, 5e-9	
TXA	varies	
PCI	9.00E-08	[63]
APnc	3.50E-07	[78]
A2M	0, 3.4e-6	[81]
A1AT	0, 3.5e-5	[81]

[1]If unlisted, initial value is zero

[2]Units are in M

Bibliography

[1] D. Hoyert and J. Xu, *National Vital Statistics Reports: Deaths: Preliminary Data for 2011*, *National vital statistics reports* **61** (2012), no. 6.

[2] K. Brohi, J. Singh, M. Heron, and T. Coats, *Acute traumatic coagulopathy.*, *The Journal of trauma* **54** (2003) 1127–1130.

[3] A. Godier and S. Susen, *Trauma-induced coagulopathy*, *Annales Francaises d'Anesthesie et de Reanimation* **32** (2013) 527–530.

[4] I. Roberts, H. Shakur, T. Coats, B. Hunt, E. Balogun, L. Barnetson, L. Cook, T. Kawahara, P. Perel, D. Prieto-Merino, M. Ramos, J. Cairns, and C. Guerriero, *The CRASH-2 trial: A randomised controlled trial and economic evaluation of the effects of tranexamic acid on death, vascular occlusive events and transfusion requirement in bleeding trauma patients*, *Health Technology Assessment* **17** (2013), no. 10 1–80.

[5] N. Mackman, *Tissue-specific hemostasis in mice*, *Arteriosclerosis, Thrombosis, and Vascular Biology* **25** (2005), no. 11 2273–2281.

[6] F. Olldashi, M. Kerçi, T. Zhurda, K. Ruçi, A. Banushi, and et. al..., *The importance of early treatment with tranexamic acid in bleeding trauma patients: an exploratory analysis of the CRASH-2 randomised controlled trial*, *The Lancet* **377** (mar, 2011) 1096–1101.e2.

[7] K. Brohi, M. J. Cohen, M. T. Ganter, M. A. Matthay, R. C. Mackersie, and J.-F. Pittet, *Acute traumatic coagulopathy: initiated by hypoperfusion: modulated through the protein C pathway?*, *Annals of surgery* **245** (2007) 812–818.

[8] B. H. Shaz, A. M. Winkler, A. B. James, C. D. Hillyer, and J. B. Macleod, *Pathophysiology of early trauma-induced coagulopathy: emerging evidence for hemodilution and coagulation factor depletion.*, *The Journal of trauma* **70** (2011), no. 6 1401–1407.

[9] H. B. Moore, E. E. Moore, E. Gonzalez, K. C. Hansen, M. Dzieciatkowska, M. P. Chapman, A. Sauaia, B. West, A. Banerjee, and C. C. Silliman, *Hemolysis exacerbates hyperfibrinolysis, whereas platelolysis shuts down fibrinolysis: evolving*

concepts of the spectrum of fibrinolysis in response to severe injury., *Shock (Augusta, Ga.)* **43** (2015), no. 1 39–46.

[10] M. P. Chapman, E. E. Moore, H. B. Moore, E. Gonzalez, F. Gamboni, J. G. Chandler, S. Mitra, A. Ghasabyan, T. L. Chin, A. Sauaia, A. Banerjee, and C. C. Silliman, *Overwhelming tPA release, not PAI-1 degradation, is responsible for hyperfibrinolysis in severely injured trauma patients.*, *The journal of trauma and acute care surgery* **80** (2016), no. 1 15–16.

[11] A. Y. Mitrophanov, A. S. Wolberg, and J. Reifman, *Kinetic model facilitates analysis of fibrin generation and its modulation by clotting factors: implications for hemostasis-enhancing therapies*, *Mol. BioSyst.* **10** (2014), no. 9 2347–2357.

[12] A. Y. Mitrophanov, F. R. Rosendaal, and J. Reifman, *Computational analysis of intersubject variability and thrombin generation in dilutional coagulopathy.*, *Transfusion* **52** (nov, 2012) 2475–86.

[13] V. Govindarajan, V. Rakesh, J. Reifman, and A. Y. Mitrophanov, *Computational Study of Thrombus Formation and Clotting Factor Effects under Venous Flow Conditions*, *Biophysical Journal* **110** (2016), no. 8 1869–1885.

[14] A. Y. Mitrophanov, F. R. Rosendaal, and J. Reifman, *Therapeutic correction of thrombin generation in dilution-induced coagulopathy: computational analysis based on a data set of healthy subjects.*, *The journal of trauma and acute care surgery* **73** (2012), no. 2 Suppl 1 S95—-S102.

[15] M. F. Hockin, K. C. Jones, S. J. Everse, and K. G. Mann, *A model for the stoichiometric regulation of blood coagulation.*, *J. Biol. Chem.* **277** (may, 2002) 18322–18333.

[16] B. E. Bannish, J. P. Keener, and A. L. Fogelson, *Modelling fibrinolysis: a 3D stochastic multiscale model.*, *Mathematical medicine and biology : a journal of the IMA* **31** (mar, 2014) 17–44.

[17] M. C. Bravo, T. Orfeo, K. G. Mann, and S. J. Everse, *Modeling of human factor Va inactivation by activated protein C.*, *BMC systems biology* **6** (2012) 45.

[18] A. L. Fogelson and K. B. Neeves, *Fluid Mechanics of Blood Clot Formation*, *Annual Review of Fluid Mechanics* **47** (2015), no. 1 377–403.

[19] M. K. Runyon, C. J. Kastrup, B. L. Johnson-Kerner, T. G. V. Ha, and R. F. Ismagilov, *Effects of shear rate on propagation of blood clotting determined using microfluidics and numerical simulations.*, *J. Am. Chem. Soc.* **130** (mar, 2008) 3458–3464.

[20] K. Leiderman and A. L. Fogelson, *Grow with the flow: a spatial-temporal model of platelet deposition and blood coagulation under flow.*, *Math. Med. Biol.* **28** (mar, 2011) 47–84.

[21] M. S. Chatterjee, W. S. Denney, H. Jing, and S. L. Diamond, *Systems Biology of Coagulation Initiation: Kinetics of Thrombin Generation in Resting and Activated Human Blood*, *PLoS Computational Biology* **6** (sep, 2010) e1000950.

[22] B. E. Bannish, J. P. Keener, M. Woodbury, J. W. Weisel, and A. L. Fogelson, *Modelling fibrinolysis: 1D continuum models.*, *Mathematical medicine and biology : a journal of the IMA* **31** (mar, 2014) 45–64.

[23] S. Butenas, B. a. Bouchard, K. E. Brummel-Ziedins, B. Parhami-Seren, and K. G. Mann, *Tissue factor activity in whole blood.*, *Blood* **105** (apr, 2005) 2764–70.

[24] K. E. Brummel-Ziedins, T. Orfeo, P. W. Callas, M. Gissel, K. G. Mann, and E. G. Bovill, *The Prothrombotic Phenotypes in Familial Protein C Deficiency Are Differentiated by Computational Modeling of Thrombin Generation*, *PLoS ONE* **7** (sep, 2012) e44378.

[25] C. Zamarron, H. R. Lijnen, and D. Collen, *Kinetics of the activation of plasminogen by natural and recombinant tissue-type plasminogen activator*, *Journal of Biological Chemistry* **259** (1984), no. 4 2080–2083.

[26] van Hinsbergh VWM, *Regulation of the synthesis and secretion of plasminogen activators by endothelial cells*, *Pathophysiology of Haemostasis and Thrombosis* **18** (1988), no. 4-6 307–327, [1011.1669].

[27] Y. van den Eijnden-Schrauwen, T. Kooistra, R. E. de Vries, and J. J. Emeis, *Studies on the acute release of tissue-type plasminogen activator from human endothelial cells in vitro and in rats in vivo: evidence for a dynamic storage pool.*, *Blood* **85** (1995), no. 12 3510–3517.

[28] J. J. Emeis, Y. Van Den Eijnden-Schrauwen, C. M. Van Den Hoogen, W. De Priester, a. Westmuckett, and F. Lupu, *An endothelial storage granule for tissue-type plasminogen activator*, *Journal of Cell Biology* **139** (1997), no. 1 245–256.

[29] A. L. Fogelson and N. Tania, *Coagulation under flow: the influence of flow-mediated transport on the initiation and inhibition of coagulation.*, *Pathophysiol. Haemost. Thromb.* **34** (jan, 2005) 91–108.

[30] M. E. Young, P. A. Carroad, and R. L. Bell, *Estimation of diffusion coefficients of proteins*, *Biotechnology and Bioengineering* **22** (1980), no. 5 947–955.

[31] D. N. Naumann, J. Hazeldine, M. J. Midwinter, S. D. Hutchings, and P. Harrison, *Poor microcirculatory flow dynamics are associated with endothelial cell damage and glycocalyx shedding after traumatic hemorrhagic shock*, *Journal of Trauma and Acute Care Surgery* **84** (jan, 2018) 81–88.

[32] J. J. Emeis, *Regulation of the acute release of tissue-type plasminogen activator from the endothelium by coagulation activation products*, *Annals of the New York Academy of Sciences* **667** (1992) 249–258.

[33] M. a. Gimbrone, R. S. Cotran, and J. Folkman, *Human vascular endothelial cells in culture. Growth and DNA synthesis.*, *The Journal of cell biology* **60** (1974) 673–84, [1011.1669].

[34] V. W. van Hinsbergh, T. Kooistra, E. A. van den Berg, H. M. Princen, W. Fiers, and J. J. Emeis, *Tumor necrosis factor increases the production of plasminogen activator inhibitor in human endothelial cells in vitro and in rats in vivo*, *Blood* **72** (nov, 1988) 1467 LP – 1473.

[35] B. Huebner, E. E. Moore, H. B. Moore, M. Kelher, A. Banerjee, E. D. Peltz, and C. C. Silliman, *Thrombin Provokes PAI-1 Release from Platelets*, *Journal of the American College of Surgeons* **223** (2016), no. 4 S159.

[36] A. Kuharsky and A. Fogelson, *Surface-mediated control of blood coagulation: the role of binding site densities and platelet deposition*, *Biophysical Journal* **80** (mar, 2001) 1050–74.

[37] M. Hoylaerts, D. C. Rijken, H. R. Lijnen, and D. Collen, *Kinetics of the activation of plasminogen by human tissue plasminogen activator. Role of fibrin*, *Journal of Biological Chemistry* **257** (1982), no. 6 2912–2919.

[38] P. L. McCormack, *Tranexamic Acid*, *Drugs* **72** (mar, 2012) 585–617.

[39] N. Hijazi, R. Abu Fanne, R. Abramovich, S. Yarovoi, M. Higazi, S. Abdeen, M. Basheer, E. Maraga, D. B. Cines, and A. A.-R. Higazi, *Endogenous plasminogen activators mediate progressive intracranial hemorrhage after traumatic brain injury.*, *Blood* **125** (2015), no. 16 2558–2567.

[40] I. Raza, R. Davenport, C. Rourke, S. Platton, J. Manson, C. Spoors, S. Khan, H. D. De'Ath, S. Allard, D. P. Hart, K. J. Pasi, B. J. Hunt, S. Stanworth, P. K. Maccallum, and K. Brohi, *The incidence and magnitude of fibrinolytic activation in trauma patients*, *Journal of Thrombosis and Haemostasis* **11** (2013), no. 2 307–314, [NIHMS150003].

[41] D. H. Jenkins, J. F. Rappold, J. F. Badloe, O. Berséus, L. Blackbourne, K. H. Brohi, F. K. Butler, A. P. Cap, M. J. Cohen, R. Davenport, M. DePasquale,

H. Doughty, E. Glassberg, T. Hervig, T. J. Hooper, R. Kozar, M. Maegele, E. E. Moore, A. Murdock, P. M. Ness, S. Pati, T. Rasmussen, A. Sailliol, M. A. Schreiber, G. A. Sunde, L. M. G. van de Watering, K. R. Ward, R. B. Weiskopf, N. J. White, G. Strandenes, and P. C. Spinella, *Trauma hemostasis and oxygenation research position paper on remote damage control resuscitation: definitions, current practice, and knowledge gaps.*, *Shock (Augusta, Ga.)* **41 Suppl 1** (2014) 3–12, [NIHMS150003].

[42] T. Toung, P. M. Reilly, K. C. Fuh, R. Ferris, and G. B. Bulkley, *Mesenteric vasoconstriction in response to hemorrhagic shock*, *Shock* **13** (2000), no. 1073-2322 267–273.

[43] H. C. Wiggers, R. C. Ingraham, F. Roemhild, and H. Goldberg, *Vasoconstriction and the development of irreversible hemorrhagic shock*, *American Journal of Physiology–Legacy Content* **153** (1948), no. 3 511–520.

[44] S. R. Fraser, N. A. Booth, and N. J. Mutch, *The antifibrinolytic function of factor XIII is exclusively expressed through α2-antiplasmin cross-linking*, *Blood* **117** (2011), no. 23 6371–6374.

[45] Y. Sakata and N. Aoki, *Significance of cross-linking of α2-plasmin inhibitor to fibrin in inhibition of fibrinolysis and in hemostasis*, *Journal of Clinical Investigation* **69** (1982), no. 3 536–542.

[46] J. W. Jansen, F. Haverkate, J. Koopman, H. K. Nieuwenhuis, C. Kluft, and T. A. Boschman, *Influence of factor XIIIa activity on human whole blood clot lysis in vitro*, *Thromb.Haemost.* **57** (1987), no. 0340-6245 (Print) 171–175.

[47] B. M. Howard, L. Z. Kornblith, C. K. Cheung, M. E. Kutcher, B. Y. Miyazawa, R. F. Vilardi, and M. J. Cohen, *Inducing Acute Traumatic Coagulopathy In Vitro : The Effects of Activated Protein C on Healthy Human Whole Blood*, .

[48] H. M. Kang, M. H. Kalnoski, M. Frederick, and W. L. Chandler, *The kinetics of plasmin inhibition by aprotinin in vivo*, *Thrombosis Research* **115** (2005), no. 4 327–340.

[49] A. P. Cap, D. G. Baer, J. A. Orman, J. Aden, K. Ryan, and L. H. Blackbourne, *Tranexamic Acid for Trauma Patients: A Critical Review of the Literature*, *The Journal of Trauma: Injury, Infection, and Critical Care* **71** (jul, 2011) S9–S14.

[50] H. Schöchl, C. J. Schlimp, and M. Maegele, *Tranexamic Acid, Fibrinogen Concentrate, and Prothrombin Complex Concentrate*, *Shock* **41** (may, 2014) 44–46.

[51] J. A. Williams-Johnson, A. H. McDonald, G. G. Strachan, and E. W. Williams, *Effects of tranexamic acid on death, vascular occlusive events, and blood*

transfusion in trauma patients with significant haemorrhage (CRASH-2): a randomised, placebo-controlled trial, *The Lancet* **376** (jul, 2010) 23–32.

[52] M. P.L., *Tranexamic Acid: A review of its use in the treatment of hyperfibrinolysis*, *Drugs* **72** (2012), no. 5 585–617.

[53] A. Takada and Y. Takada, *Conversion of glu-plasminogen to plasmin by urokinase in the presence of tranexamic acid*, *Thrombosis Research* **22** (1981), no. 4 437–443.

[54] N. Hijazi, R. Abu Fanne, R. Abramovitch, S. Yarovoi, M. Higazi, S. Abdeen, M. Basheer, E. Maraga, D. B. Cines, and A. Al-Roof Higazi, *Endogenous plasminogen activators mediate progressive intracerebral hemorrhage after traumatic brain injury in mice*, *Blood* **125** (apr, 2015) 2558–2567.

[55] J. L. Saes, S. E. M. Schols, W. L. van Heerde, and M. R. Nijziel, *Hemorrhagic disorders of fibrinolysis: a clinical review*, *Journal of Thrombosis and Haemostasis* **16** (aug, 2018) 1498–1509.

[56] V. Ellis, N. Behrendt, and K. Dano, *Plasminogen activation by receptor-bound urokinase: A kinetic study with both cell-associated and isolated receptor*, *Journal of Biological Chemistry* **266** (1991), no. 19 12752–12758.

[57] M. Hoylaerts, H. R. Lijnen, and D. Collen, *Studies on the mechanism of the antifibrinolytic action of tranexamic acid*, *BBA - General Subjects* **673** (1981), no. C 75–85.

[58] C. Longstaff and M. Locke, *Increased urokinase and consumption of α 2 âĂŘantiplasmin as an explanation for the loss of benefit of tranexamic acid after treatment delay*, *Journal of Thrombosis and Haemostasis* (dec, 2018) jth.14338.

[59] D. M. Wootton, A. S. Popel, and B. Rita Alevriadou, *An experimental and theoretical study on the dissolution of mural fibrin clots by tissue-type plasminogen activator*, *Biotechnology and Bioengineering* **77** (feb, 2002) 405–419.

[60] T. B. Wu, S. Wu, M. Buoni, T. Orfeo, K. Brummel-Ziedins, M. Cohen, and L. Petzold, *Computational Model for Hyperfibrinolytic Onset of Acute Traumatic Coagulopathy*, *Annals of Biomedical Engineering* **46** (aug, 2018) 1173–1182.

[61] M. M. C. G. SILVA, C. THELWELL, S. C. WILLIAMS, and C. LONGSTAFF, *Regulation of fibrinolysis by C-terminal lysines operates through plasminogen and plasmin but not tissue-type plasminogen activator*, *Journal of Thrombosis and Haemostasis* **10** (nov, 2012) 2354–2360.

[62] D. C. Stump, M. Thienpont, and D. Collen, *Purification and characterization of a novel inhibitor of urokinase from human urine. Quantitation and preliminary characterization in plasma.*, *The Journal of biological chemistry* **261** (sep, 1986) 12759–66.

[63] M. J. Heeb, F. España, M. Geiger, D. Collen, D. C. Stump, and J. H. Griffin, *Immunological identity of heparin-dependent plasma and urinary protein C inhibitor and plasminogen activator inhibitor-3.*, *The Journal of biological chemistry* **262** (nov, 1987) 15813–6.

[64] K. Kolev, I. Léránt, K. Tenekejiev, and R. Machovich, *Regulation of fibrinolytic activity of neutrophil leukocyte elastase, plasmin, and miniplasmin by plasma protease inhibitors.*, *The Journal of biological chemistry* **269** (jun, 1994) 17030–4.

[65] L. Martos, L. A. Ramón, J. Oto, Á. Fernández-Pardo, S. Bonanad, A. R. Cid, A. Gruber, J. H. Griffin, F. España, S. Navarro, and P. Medina, *α 2 -Macroglobulin Is a Significant in Vivo Inhibitor of Activated Protein C and Low APC:α 2 M Levels Are Associated with Venous Thromboembolism*, *Thrombosis and Haemostasis* **118** (2018), no. 4 630–638.

[66] K. Brohi, M. J. Cohen, M. T. Ganter, M. J. Schultz, M. Levi, R. C. Mackersie, and J.-F. Pittet, *Acute coagulopathy of trauma: hypoperfusion induces systemic anticoagulation and hyperfibrinolysis.*, *The Journal of trauma* **64** (may, 2008) 1211–7; discussion 1217.

[67] J. F. Holmes, *Effects of Delaying Fluid Resuscitation on an Injury to the Systemic Arterial Vasculature*, *Academic Emergency Medicine* **9** (apr, 2002) 267–274.

[68] H. P. Santry and H. B. Alam, *FLUID RESUSCITATION*, *Shock* **33** (mar, 2010) 229–241.

[69] L. Kuepfer, C. Niederalt, T. Wendl, J.-F. Schlender, S. Willmann, J. Lippert, M. Block, T. Eissing, and D. Teutonico, *Applied Concepts in PBPK Modeling: How to Build a PBPK/PD Model*, *CPT: Pharmacometrics & Systems Pharmacology* **5** (oct, 2016) 516–531.

[70] S. Balay, S. Abhyankar, M. F. Adams, J. Brown, P. Brune, K. Buschelman, L. Dalcin, V. Eijkhout, W. D. Gropp, D. Kaushik, M. G. Knepley, D. A. May, L. C. McInnes, K. Rupp, B. F. Smith, S. Zampini, H. Zhang, and H. Zhang, "PETSc Web page." `http://www.mcs.anl.gov/petsc`, 2017.

[71] M. C. Naski and J. a. Shafer, *A kinetic model for the alpha-thrombin-catalyzed conversion of plasma levels of fibrinogen to fibrin in the presence of antithrombin III.*, *The Journal of biological chemistry* **266** (1991), no. 20 13003–10.

[72] M. Schneider, N. Brufatto, E. Neill, and M. Nesheim, *Activated Thrombin-activatable Fibrinolysis Inhibitor Reduces the Ability of High Molecular Weight Fibrin Degradation Products to Protect Plasmin from Antiplasmin*, *Journal of Biological Chemistry* **279** (2004), no. 14 13340–13345.

[73] P. Y. Kim, R. J. Stewart, S. M. Lipson, and M. E. Nesheim, *The relative kinetics of clotting and lysis provide a biochemical rationale for the correlation between elevated fibrinogen and cardiovascular disease*, *Journal of Thrombosis and Haemostasis* **5** (2007), no. 6 1250–1256.

[74] C. M. Hekman Loskutoff, D. J., *Kinetic Analysis of the Interactions between Plasminogen Activator Inhibitor 1 and both Urokinase and Tissue Plasminogen Activator*, *Arch. Biochem. Biophys.* **262** (1988), no. 1 199–210.

[75] A. J. G. Horrevoets, H. Pannekoek, and M. E. Nesheim, *A steady-state template model that describes the kinetics of fibrin- stimulated [Glu1]- and [Lys78]plasminogen activation by native tissue- type plasminogen activator and variants that lack either the finger or kringle-2 domain*, *Journal of Biological Chemistry* **272** (1997), no. 4 2183–2191.

[76] A. J. G. Horrevoets, *Plasminogen activator inhibitor 1 (PAI-1): In vitro activities and clinical relevance*, *British Journal of Haematology* **125** (2004), no. 1 12–23.

[77] F. J. Castellino and J. R. Powell, *[29] Human plasminogen*, pp. 365–378. 1981.

[78] S. Abdul, F. W. Leebeek, D. C. Rijken, and S. U. De Willige, *Natural heterogeneity of α2-antiplasmin: Functional and clinical consequences*, *Blood* **127** (2016), no. 5 538–545.

[79] K. E. Brummel, S. Butenas, and K. G. Mann, *An integrated study of fibrinogen during blood coagulation 6*, *J Biol.Chem.* **274** (1999), no. 0021-9258 (Print) 22862–22870.

[80] D. C. RIJKEN and H. R. LIJNEN, *New insights into the molecular mechanisms of the fibrinolytic system*, *Journal of Thrombosis and Haemostasis* **7** (jan, 2009) 4–13.

[81] M. Levi, D. Roem, A. Kamp, J. de Boer, C. Hack, and J. ten Cate, *Assessment of the Relative Contribution of Different Protease Inhibitors to the Inhibition of Plasmin In Vivo*, *Thrombosis and Haemostasis* **69** (feb, 1993) 141–146.